Theoretical Notes
Note L80

SPECIAL PROJECTS-30
1972

UNITED STATES
DEPARTMENT OF THE INTERIOR
GEOLOGICAL SURVEY

Federal Center, Denver, Colorado 80225

EMPIRICAL PREDICTIVE CURVES FOR RESISTIVITY AND DIELECTRIC CONSTANT OF EARTH MATERIALS: 100 Hz to 100 MHz

By

R. C. Bigelow and W. R. Eberle

CONTENTS

ILLUSTRATIONS

ILLUSTRATIONS

TABLES

UNITED STATES
DEPARTMENT OF THE INTERIOR
GEOLOGICAL SURVEY

Special Projects-30
1972

Federal Center, Denver, Colorado 80225

EMPIRICAL PREDICTIVE CURVES FOR RESISTIVITY AND DIELECTRIC CONSTANT OF EARTH MATERIALS: 100 Hz to 100 MHz

By

R. C. Bigelow and W. R. Eberle

ABSTRACT

The variation or dispersion with frequency of nonmetallic earth material resistivities and dielectric constants can be predicted in the frequency range 100 Hz to 100 MHz by the use of empirical curves derived from measured data on sandstones. Laboratory measurements of resistivity and dielectric constant in the stated frequency range are reported for the upper sandstone bed in the Sunnyside Member of Blackhawk Formation, the Lyons Sandstone, and the sandstone bed of the Laramie Formation. Samples of the sandstones were fully or partially saturated with saline solutions whose resistivities were ρ_w = 0.3, 1.0, 3.0, 10, 30, and 100 ohm-meters. Porosities of the sandstones were ϕ = 0.230, 0.209, and 0.255, respectively.

The data were examined to determine the relationships between porosity, fractional water content, clay content, water resistivity, ρ_w, and the dispersions of resistivity and dielectric constant with frequency. For each sandstone, the dispersions of resistivity of fully and partially saturated samples are the same, within experimental error, when the resistivities of the samples are equal at low frequencies ($\leq$ 100 Hz). All three sandstones, when fully saturated with water of a

given ρ_w, exhibit the same dispersion of resistivity. Clay in the pore spaces of an earth material affects the shape of the dispersion curve when ρ_w is $\geq$ 10 ohm-meters but has little effect when ρ_w = 1.0 ohm-meter. On the basis of the foregoing observations, a set of normalized resistivity versus frequency curves are constructed which can be used to predict the frequency dependence of resistivity in nonmetallic earth materials and instructions for their use are given.

At frequencies below 1 MHz, the dielectric constant of an earth material is proportional to the quantity $\kappa'' = (2\pi f \varepsilon_o \rho)^{-1}$ where f, ε_o and ρ are the frequency, permittivity of free space, and resistivity of the material, respectively; the proportionality depends strongly on ρ_w but not on the porosity or state of saturation of the material.

Plots of dielectric constant versus κ'' are used to predict the dielectric constant of an earth material when its resistivity is known at the same frequency. At 10 and 100 MHz, the dielectric constant approaches a constant that is determined in part by the nature of the earth material; the accuracy of the dielectric constant prediction curves is diminished at those frequencies. Two curves that are based on a logarithmic mixing formula, empirically relate the fractional water content and the porosity of an earth material to the dielectric constant at 100 MHz to provide an improved estimate of dielectric constant at 100 MHz.

INTRODUCTION

A series of laboratory investigations have been undertaken by the U.S. Geological Survey (USGS) on behalf of the Air Force Weapons Laboratories (AFWL) to determine to what extent and under what conditions the frequency dependence of the electrical properties of earth materials can be predicted in the range 100 Hz to 100 MHz. This report contains an account of those investigations and the predictive information obtained from them.

At any given frequency, f, the electrical properties of an earth material can be described by two parameters: the resistivity, ρ, and the relative dielectric constant, κ, of the material. That both ρ and κ of earth materials show variation with frequency (called dispersion) was first indicated by the work of Smith-Rose (1933) on soils and was later substantiated in laboratory studies of other earth materials by other investigators (Scott and others, 1967). Extensive reference bibliographies are found in review papers by Emerson (1969) and Ward and Fraser (1968).

The plots in figure 1 illustrate dispersion of resistivity and dielectric constant for a "typical" moist earth material such as a soil. Three properties that are common to many earth materials are illustrated by the curves. First, the resistivity usually decreases very slightly between low frequencies ($\leq$100 Hz) and approximately 1 MHz; above 1 MHz, resistivity drops more rapidly with increasing frequency. Second, the dielectric constant is often extremely large, between 10^4 and 10^6 at 100 Hz, and decreases with

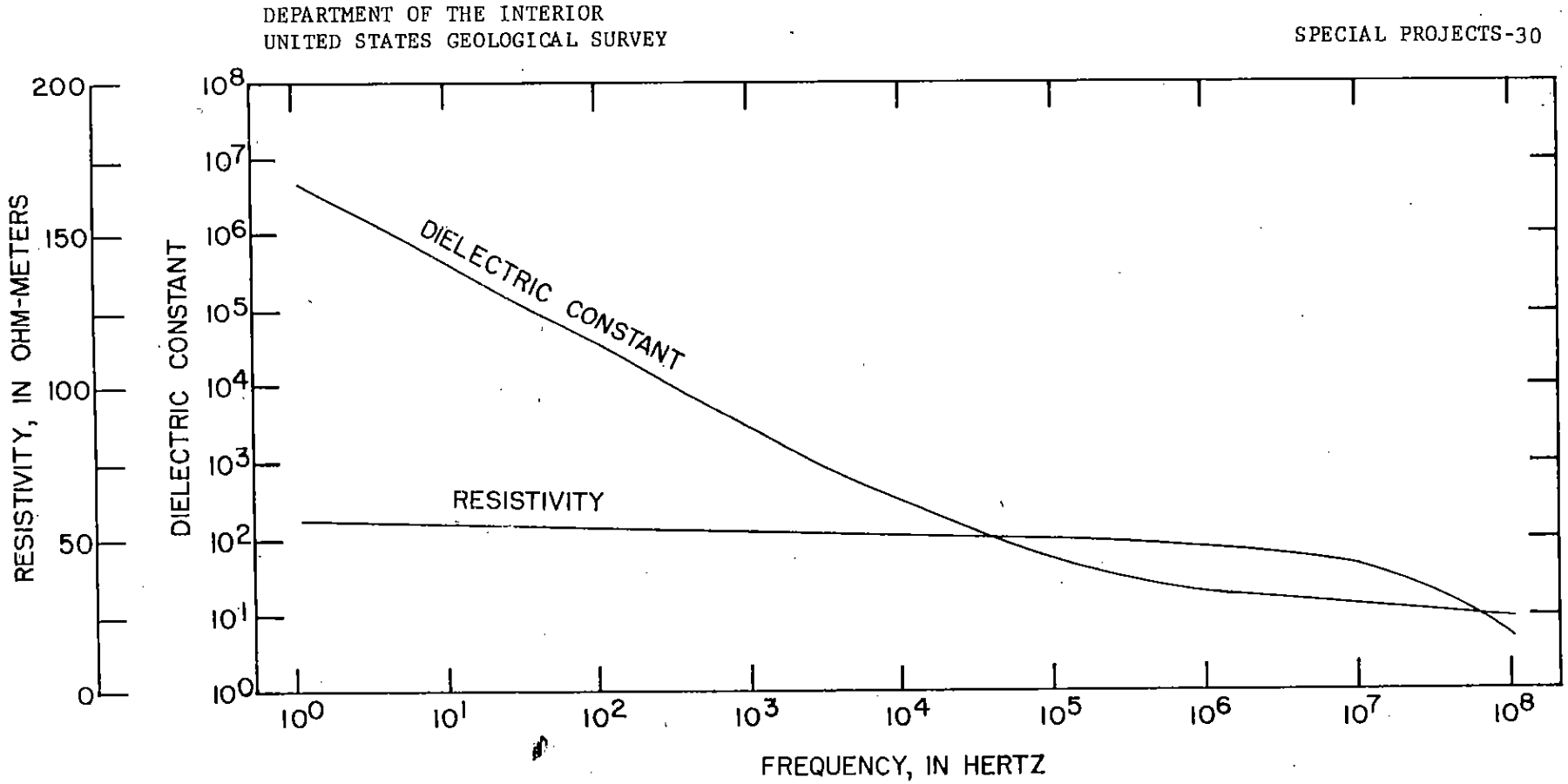

Figure 1.--Resistivity and dielectric constant as a function of frequency for a typical earth material

increasing frequency at the rate of about one decade per decade of frequency. Near 1 MHz, the dielectric constant dispersion curve undergoes a transition and flattens out with increasing frequency. Third, the frequency range in which the maximum dispersion of resistivity occurs usually lies above the range of maximum dispersion of dielectric constant (Arulanandan and Mitchell, 1968).

Most of the studies of dispersion of resistivity and dielectric constants have been made in laboratories rather than in the field. Experimental conditions are harder to control and instrumentation for measurements at several frequencies is more difficult in the field than in the laboratory. However, Grubb and Wait (1971) have recently measured ρ and κ for materials in the field at frequencies between 1 and 10 MHz. In support of their effort samples of the same materials were measured within the same frequency range by the USGS. The dispersions of ρ and of κ observed in the laboratory are substantially the same as those observed in the field (Grubb and Wait, 1971) which indicates that the laboratory determinations of dispersion are substantially correct. Because measurements of resistivity and dielectric constant are much more difficult in the field than in the laboratory the present investigation was undertaken to find methods by which in situ electrical properties can be predicted in the frequency range 100 Hz to 100 MHz.

This report includes a qualitative theoretical discussion of conduction and polarization mechanisms in earth materials. Some useful empirical relationships between resistivity at low frequencies

($\lesssim$100 Hz) and the physical properties of earth materials are introduced. The Experimental Methods section (p. 16) contains a discussion of the rationale that underlies the use of sandstones as model earth materials and a description of the three sandstones used in the experiments. Most of the experimental procedure has been explained in previous reports and a companion report reviewing laboratory methods is in preparation by the authors; therefore, only a brief description of the experimental technique is included here.

Electrical measurements that were made on each of the sandstones are summarized in two tables in the Data and Results section (p. 21) and the data are tabulated in the Appendix. In a Predictive Curves, Derivation section, (p. 30) the data are analyzed to determine what electrical properties the three sandstones have in common. From these properties three sets of curves are constructed that permit the resistivity and dielectric constant of an earth material to be predicted as a function of frequency. The use and limitations of the predictive curves are explained, for convenience, in a separate section (p. 48) which concludes the body of the report.

THEORETICAL BACKGROUND

Electrical effects of water and salts

The type of behavior exhibited in figure 1 is characteristic of earth materials that contain moisture. Totally dry earth materials have resistivities in the megohm-meter range at low frequencies (Khalafalla, 1971) and their resistivities vary approximately as inverse frequency (Fuller and Ward, 1969). The dielectric constants of dry

materials are almost independent of frequency and have values of the order of 20 or less according to data in Bondarenko's (1965) paper. The latter reference also shows that water contents of less than 1 percent can cause dispersion in dielectric constant approaching that of figure 1 while Valeev and Parkhomenko (1965) show that the resistive dispersion observed in dry rock for moisture contents of a few percent almost disappears at low frequencies.

Many earth materials contain voids or microfractures, called pores, that are connected. When a material is wetted, its pore spaces are invaded by water. When the water contains soluble ions, as is usual in nature, a conductive electrolyte is formed. Thus, the electrical properties of many earth materials are determined by electrolytic conduction through the pores and not by conduction through the earth material itself. The case of electron conductance through metallic minerals is an exception that is not considered here; it is discussed by Ward and Fraser (1968).

The amount of water in the pores of an earth material, the ionic concentration in the water, the geometry of the matrix, and the clay particles and native salts in the pores all influence the electrical properties of an earth material. The effects of these influences are often described in terms of the following parameters: the porosity, ϕ, defined as the ratio of total void space to the volume of the material; the volume fraction, S_w, defined as pore space occupied by water; the clay content; and the ion concentration in the pore water. If the ions are from salts, salinity is a proper measure of ion content. However,

it is often convenient to specify the resistivity of a saline solution rather than the salinity itself as an indication of ion content because the resistivity of the solution is easily measured. The water resistivity, ρ_w, and salinity of a solution are approximately inversely related; high resistivities imply low salinities and vice versa. If an earth material that is free of native salts is placed in contact with an aqueous saline solution, the pore-water resistivity will not generally be the same as ρ_w because of the effects of clay in the earth material.

Electrical effects of clay

The role of clay in rocks and soils has received extensive attention in the literature (Winsauer and McCardell, 1953; Madden and Marshall, 1958, 1959a, 1959b; Keller and Licastro, 1959; Howell and Licastro, 1961, Wyllie, 1963; Ward and Fraser, 1968; Arulanandan and Mitchell, 1968). When present, clays play a dominant role in the electrical properties of wet rock because they are capable of cation exchange. The metallic ion of a dissolved salt, for instance sodium from sodium chloride, can exchange with a metallic ion in a clay's crystalline lattice. When a particle of clay "charged" with sodium is placed in contact with water, the sodium ions desorb from the structure and form a cationic cloud around the now negatively charged clay particle.

A computation in Keller and Frischknecht (1966) illustrates the effect of clay content on the pore-water resistivity of a sandstone having 20 percent porosity when the sandstone contains 0.1 percent

montmorillonite by weight. If the clay is fully sodium charged and the rock is saturated with distilled water (180 kilohm-meter resistivity), the resistivity of the water in the pores decreases to 6 ohm-meters when the clay desorbs its sodium ions. As Keller and Frischknecht point out, the computation somewhat overstates the effect of clays because montmorillonite has a much larger exchange capacity than other clays and, more importantly, the resistivity after desorbtion is computed as if the ions are distributed uniformly throughout the pore water and have their normal mobility. On the contrary, the ions are concentrated in the vicinity of the clay particles and their motion is hindered by the presence of the charged clay particles. Nonetheless, clay disseminated in the pore space strongly depresses the effective pore-water resistivity.

Clays affect the effective dielectric constants of earth materials as well as their resistivities. The ionic cloud around a clay particle and the particle itself form an electric dipole that polarizes when an electric field is applied. Clays also give rise to a phenomenon known as membrane polarization.

Polarization theory

Madden and Marshall (1958, 1959a, 1959b) propose a membrane polarization theory to account for the size and dispersion of the dielectric constant of earth materials at low frequencies. According to Madden and Marshall, the positive ion cloud around a clay particle in a pore space can act as a selective filter for diffusing free ions, permitting the positive ions (cations) to pass but blocking the negative ions (anions). If clay is distributed discontinuously along a

pore path and an electric field is causing free ions to drift, alternating concentrations of positive and negative ions can accumulate between the clay particles causing a large polarization to build up. The polarization build up is diffusion-rate limited and a rapidly alternating field causes less polarization than a slowly alternating one; thus, polarization decreases with increasing frequency. Further information on membrane polarization is found in Ward and Fraser (1968).

Several authors, for instance Arulanandan and Mitchell (1968), and Khalafalla (1971), have attemped to use Debye relaxation time theory to explain the polarization phenomenon in rock; the theory is reviewed in Von Hippel (1954). Debye's theory envisions electrical dipoles rotating in a viscous medium under the influence of an electric field. If an array of dipoles is alined in a viscous dielectric medium and the field causing the alinement of the dipoles is switched off, thermal effects will randomize the dipoles in a characteristic relaxation time. The dispersion of resistivity and dielectric constant for the material containing the dipoles can be predicted from a knowledge of the relaxation time. In practice, the theory is turned around and the known resistivity and dielectric constant information is utilized to determine the relaxation time. In the case of earth materials, the analysis requires the assumption of a spectrum of relaxation times (for instance, Khalafalla, 1971) to explain the data; this feature limits the usefulness of the theory.

In the derivation of the relaxation theory (Von Hippel, 1954), the electrical parameters are converted into units having the same dimensions. One such set of parameters is the real and imaginary part of the complex dielectric constant. A complex dielectric constant is defined by the equation

$$\kappa' = \kappa + j\kappa'' \qquad (1)$$

where κ is the usual dielectric constant and κ'' is related to the bulk resistivity of the material by

$$\kappa'' = (2\pi f \varepsilon_o \rho)^{-1}$$

where ε_o is the permittivity of free space. These parameters prove to be useful in analyzing the present data.

Ionic interactions in the pore space

For present purposes, only a qualitative physical picture of the action of ions in the interior of wet rock is needed. Conduction takes place by means of free ions in the pore water and is affected by layers of ions that cluster around clay particles. Under an applied direct-current or low audio range alternating current field, the ions drift and diffuse; in this frequency range, the Madden and Marshall (1958, 1959a, 1959b) ion-filter polarization theories ought to apply if clay particles exist within the pore spaces. The diffusion rate and mobility of the free ions will vary with ionic species and pore size. Ions in layers will drift more slowly, on the average, than the free ions and will have mobilities that depend on the potentials by which they are bound.

As the frequency increases, the excursion of any one ion during one-half cycle must decrease, thermal effects aside, because of the inertia and limited mobility of the ions. Thus, the number of collisions suffered by the ion decreases as the frequency increases and the ions tend to oscillate about fixed positions. At extremely high frequencies only the thermal agitation causes collisions, the oscillations caused by the electric field are too small to induce collision.

This physical picture, while far from complete, suggests that both the dielectric constant and the loss (resistivity) will decrease with increasing frequency. As the ionic displacements decrease the induced dipole moment does also; as the number of collisions decrease, so do losses.

Empirical relationships

Although the origin of the resistivity and dielectric constant dispersion phenomena in earth materials are reasonably well understood, there exists no theory, based on first principles, by which the electrical properties of rocks and soils can be predicted. There exists, however, a considerable fund of empirical knowledge about relationships between resistivity and the physical properties of earth materials.

The petroleum industry uses measurements of earth resistivity to deduce the composition and structure of geologic formations. The methods by which earth resistivities are measured are outlined in Wyllie (1963, p. 1-31), Lynch (1962, p. 107-109), and Keller and Frischknecht (1966, p. 1-60) among others. The in situ resistivities

are measured with extremely low frequency or direct-current sources; the dielectric constant is not important in oil-field exploration and no simple methods have been developed for measuring κ in situ.

On the basis of empirical evidence Archie (1942) proposed that the bulk resistivity of a formation, ρ, was related to the resistivity of the water saturating the formation ρ_w, by the equation

$$\rho/\rho_w = a\phi^{-m}$$

Both a and m are empirical constants that are characteristic of the formation; the value of a is often near unity while the value of m can range from about 1.6 to 2.3 (see, for example, table 8 in Keller and Frischknecht, 1966). Archie's law, as the equation is known, was formulated on the basis of oil-field experience in an environment where saturating water is extremely saline. In fresh water the value of m can change with increasing ρ_w (Alger, 1966).

For a typical earth material, a plot of ρ versus ρ_w will resemble those in figure 2. As ρ_w increases, the resistivity becomes asymptotic to a value that is characteristic for a given type of rock (Wyllie, 1963). The upper bound on ρ is not the dry bulk conductivity, which is several orders of magnitude higher (Khalafalla, 1971), but is the limiting value imposed by conduction along the surfaces of the pore walls and by clay material in the pores.

Wyllie (1963) extends Archie's law by empirically relating the bulk resistivity of an earth material to its porosity, clay content, and water resistivity. The resistivity of rock varies with the resistivity of the saturant in the same manner as two resistors in parallel

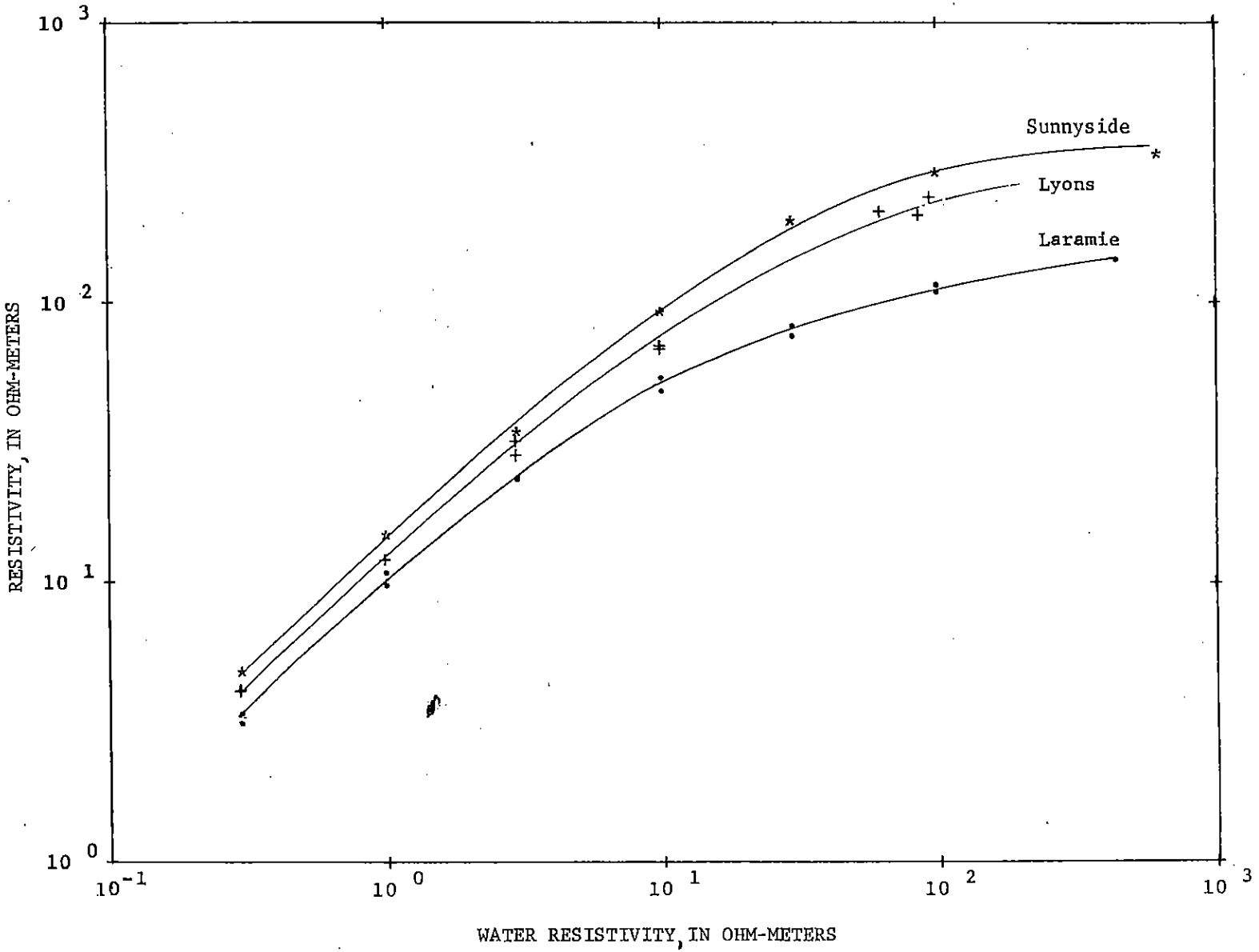

Figure 2.--Resistivity versus water resistivity for three sandstones. *, Sunnyside member of the Blackhawk Formation; +, Lyons Sandstone; •, Laramie sandstone.

if no continuous layers of clay exist in the rock. In the notation of this report:

$$(\rho)^{-1} = (\rho_w a \phi^{-m})^{-1} + (\rho_{limit})^{-1}$$

The first term on the right hand side is from Archie's law; the second is the limiting resistance owing to the presence of disseminated clay in the pore spaces. For the equation to hold, the limiting resistivity must be independent of the salinity or resistivity of the saturant, which implies that the effect of clay on resistivity is independent of the ion concentration in the saturating fluid.

Archie (1942), quoting experimental evidence from four earlier workers, suggests that the relationship between the resistivity of a partially saturated rock and the same rock fully saturated is:

$$\frac{\rho_t}{\rho} = S_w^{-n}$$

where ρ_t represents the resistivity of the partially saturated rock, ρ is the resistivity at full saturation, S_w is the fractional water content and n is an empirical constant, often assumed to be equal to two. Wyllie presents graphical evidence, however, that n can be as low as one for high-resistivity saturants in sandstone that contains clay.

Scott, Carroll, and Cunningham (1967) combine the two equations given by Archie (1942), and deduce from experiment that the most meaningful variable for determining the resistivity as a function of frequency is the total water content $S_w\phi$.

$$\rho_t = \rho_w (S_w \phi)^{-n}$$

where the two exponents, m and n, in Archie's equations are set equal and the constant, a, is taken as unity. From empirical curves and a knowledge of ($S_w\phi$), Scott, Carroll and Cunningham show that the resistivity of an earth material can be approximately predicted; they also show that resistivity and dielectric constant are empirically related for frequencies between 100 Hz and 1 MHz. The latter two facts are especially important for the present work.

EXPERIMENTAL METHODS

Experimental strategy

The empirical relationships for resistivity stress the importance of several parameters of the earth materials: the porosity, the fractional water content, and the disseminated clay content; but they do not directly involve the matrix material itself. Furthermore, Scott, Carroll, and Cunningham find empirical relationships that permit both ρ and κ to be predicted with little knowledge of the matrix material.

Because experience indicates that the composition of the matrix is secondary in determining the electrical properties of the material, it was decided to select samples from three sandstone formations as representative earth materials and to measure their resistivities and dielectric constants as a function of frequency in the range 100 Hz to 100 MHz. The porosity and clay content of each sandstone type were determined and the water resistivity and fractional water content were controlled in each measured sample. Both ρ_w and S_w were systematically varied until their effects on the dispersion phenomena were ascertained. Several relationships between the previously mentioned parameters and

dispersion were discovered and used to construct sets of curves for the prediction of dispersion of earth material resistivity and dielectric constant with frequency.

Description of sandstones

Three types of sandstone were chosen as model earth materials; each was quite porous, permeable, highly uniform in composition and density, and free of mineralization. In view of the importance of clay in determining the electrical parameters of wet rock, the clay contents were found by X-ray analysis; these properties are listed in table 1 along with the measured values of dry bulk density and porosity for each species of sandstone.

The upper sandstone bed in the Sunnyside Member of the Blackhawk Formation in eastern Utah is a brown-gray, fine-grained, well-cemented sandstone showing some evidence of bedding. Some soluble native salts are found by leaching the sandstone with distilled water. The method of leaching with distilled water is described subsequently in this section. Six samples of the Sunnyside sandstone were used in the experiments.

The Lyons Sandstone from the vicinity of Turkey Creek near Morrison, Colorado (Waagé, 1961), is a light-buff-colored sandstone with no visible iron staining; it is very fine grained and competent. By leaching with distilled water, the Lyons Sandstone proves to have much larger amounts of native soluble salts than the other two sandstones. Fourteen samples of the Lyons Sandstone were used in the present study.

Table 1.--Physical properties of sandstones

[Mineral contents listed below are estimated from X-ray diffractometer patterns by Paul D. Blackmon, Experimental Geochemistry and Mineralogy Branch, U.S. Geological Survey]

Sample name	Porosity	Dry bulk density (g/cc)	Mineral contents	Estimated amounts (percent)
Sunnyside	0.230	2.05	Quartz	>90
			Kaolinite	~5
			Illite-mica	
			Illite-montmorillonite mixed layered	
			Calcite	
Lyons	0.209	2.06	Quartz	>90
			Calcite	<1
			Dolomite	
			Kaolinite	~1
			Montmorillonite	<2
			Montmorillonite-illite mixed layered	
			Illite	
			K-feldspar	<1
Laramie	0.255	1.89	Quartz	>80
			Feldspar	<5
			Cristobalite-opaline silica	<10
			Montmorillonite	~8
			Illite-mica	
			Kaolinite	

The sandstone bed of the Laramie Formation found in the vicinity of the Arapahoe clay pits between Denver and Morrison, Colorado, contains a white-gray sandstone that is weathered and extremely friable. Some bedding is in evidence. This sandstone has the highest clay content of the three types but almost no native salts could be leached from it. It is assumed that exposure to rainwater removed the soluble salts. Twelve samples of the Laramie sandstone were used in this investigation.

Synopsis of experimental method

Only a synopsis is given here because the details of the USGS laboratory method will be set forth in a companion report in preparation by the authors. Portions of the method have already been reported in Scott, Carroll, and Cunningham (1967) and Judy and Eberle (1969).

Blocks of sandstone were core drilled to obtain 2 1/8-inch-diameter cores. Approximately 1-inch-long samples were cut from the cores so as to fit the sample holders described by Judy and Eberle (1969).

In order to control the resistivity of the pore water, it is necessary to first remove the soluble native salts from the rock so that the samples can be saturated with sodium chloride solutions of known resistivity. To remove the native salts, a sample is placed in a vacuum jar and is covered with distilled water. When the jar is evacuated, air trapped in the rock and in the water is removed by the vacuum and the rock becomes saturated with water. As the sample stands in the water, some of the native salts diffuse out of the sample causing the resistivity of the surrounding water, ρ_w, to decrease. As ρ_w can be measured by means of a conductivity cell, the change in salt levels inside the rock sample is indirectly monitored.

The leaching process is repeated daily, starting each time with fresh distilled water, and the samples remain in water overnight under vacuum. When the water resistivity stabilizes at a value well in excess of 100 ohm-meters for several leaching cycles, the samples are said to be "cleared" and are usually ready for saturation with saline solutions. As a test, some leached samples are permitted to stand in the same water for a longer period of time (as long as 2 months) to determine if sizable changes in water resistivity occur. If sizable changes do occur, it is apparent that the leaching process has not removed most of the soluble native salts.

After a sample has been cleared, it is saturated under vacuum with a sodium chloride solution having one of the following water resistivities: ρ_w = 0.3, 1.0, 3.0, 10, 30 or 100 ohm-meters. The saturation process is similar to the leaching process described above; it is terminated when the sample takes up no more salt from the solution.

To desaturate a fully saturated sandstone sample, dry disks of blotting paper are pressed against the ends of the sample and they are left in place overnight. Saturant in the pores of the sample diffuse out into the blotters until fluid equilibrium is reached. The blotters are removed and discarded and the resistivity and dielectric constant are measured over the frequency range 100 Hz to 100 MHz.

The resistivities and dielectric constants of fully or partially saturated samples are calculated from measured resistances and capacitances of the sample. A sample is mounted with electrodes in a sample holder. A Wayne Kerr model B221 audio frequency bridge is used to measure resistance and capacitance of the mounted sample at 100 Hz and

at 1 and 10 kHz and a Wayne Kerr model B601 RF bridge is used for measurements at 100 kHz. The null detector for both bridges is a Rhode and Schwartz UBM tunable indicating amplifier whose output signal is fed into a Tektronix type 513 oscilloscope. The measurements at 1, 10, and 100 MHz are made on a Hewlett-Packard model 250B R-X bridge with a self-contained null detector unit. After the measurements on the bridges, the sample is removed from the sample holder and weighed to determine its water content.

DATA AND RESULTS

Measurements on saturated sandstones

In table 2 are listed the numbers of fully saturated samples of each kind of sandstone that were electrically measured as well as the resistivities of the solutions in which the samples were saturated. The samples, except those marked in the table with an asterisk, were saturated with sodium chloride solutions. All the measured data are tabulated in the Appendix.

An asterisk in table 2 indicates a "cleared" sample that was allowed to stand in water until the resistivity of the water stabilized. At least one of the "cleared" samples of each kind of sandstone was electrically measured. The water resistivities for the tested "cleared" samples were sufficiently high for the Laramie and Sunnyside samples that most of the native salts were removed by the leaching process. The water resistivities of the "cleared" Lyons samples, dropped from values in excess of 300 ohm-meters to those shown in the table. Thus, the Lyons Sandstone samples apparently continued to retain some native

salts. Because 30 and 100 ohm-meter sodium chloride saturants would not overcome the native salt concentrations in the Lyons Sandstone samples, no measurements for those saturants are reported.

The sample preparation time was much greater than the time required to measure a sample electrically; therefore, different samples were used for each measurement. Enough samples of the Lyons and Laramie sandstones were available to permit two samples of each sandstone type to be saturated with the indicated saline solutions. Sample to sample variations were usually less than 10 percent.

Measurements on partially saturated sandstones

In table 3 is listed the resistivity of the saturating water and the percentage saturation of each electrically measured sandstone sample for which data are reported in the Appendix. The values of water resistivity listed in table 3 and in the data in the Appendix are the resistivities of the water in which the samples were initially fully saturated.

Samples of all three sandstones were desaturated from full saturation to about 60-percent saturation. The Lyons and Sunnyside samples desaturated more readily than the Laramie samples which could not be brought below 60-percent saturation by the blotter disk desaturation method. The reason for this phenomenon is unclear. The clay content of Laramie sandstone (8 percent) is approximately twice as great as in the other two types of sandstones (4 and 5 percent) and it is possible that the clays are responsible for the water retention. Both the Lyons and Sunnyside samples were desaturated to below 40 percent and one Lyons sample was desaturated to 23 percent of full saturation.

Table 2.--Resistivity of the saturating water and the number of saturated samples of each kind of sandstone that were measured

[Data on resistivity and dielectric constant are in the Appendix]

Type of sandstone	Water resistivity (ohm-meters)	Number of samples measured
Sunnyside	625	1*
	100	1
	30	1
	10	1
	3.0	1
	1	2
	0.3	2
Lyons	95	1*
	87	1*
	63	1*
	10	2
	3.0	2
	1	2
	0.3	2
Laramie	500	1*
	441	1*
	100	2
	30	2
	10	2
	3	2
	1.0	2
	0.3	2

*"Cleared" test samples saturated with water that contains residual native salts from the samples.

Table 3.--Resistivity of the saturating water and the percentage of saturation of partially saturated sandstone samples

[Each entry under percent saturation corresponds to a set of measurements of resistivity and dielectric constant reported in the Appendix]

Type of sandstone	Water resistivity (ohm-meters)	Percent saturation
Sunnyside	10	60.6, 59.1, 41, 30.8
	1.0	67, 65, 60.2, 50, 47, 38
Lyons	10	66, 39.8
	3.0	66.5, 37.2
	1.0	62.5, 32, 23
	0.3	66, 31.9
Laramie	10	92, 84, 80.6, 68
	3.0	89, 83, 68
	1.0	91, 77, 74, 63
	0.3	91, 81, 76, 69

ERROR ANALYSIS

Table 4 lists, by frequency, the estimated accuracy of the measured resistivities and dielectric constants. The origins of the measurement errors are discussed in the remainder of this section.

The resistivity and dielectric constant of the Sunnyside, Lyons, and Laramie samples were measured on the bridges at decade intervals of frequency over the range 100 Hz to 100 MHz. The frequency of oscillation was checked against an electronic counter and found to be stable after warmup to at least four significant digits.

The sodium chloride saturant electrolytes were held to within 3 percent of their nominal resistivity values: 0.3, 1.0, 3.0, 10, 30 and 100 ohm-meters, which were determined by resistivity measurements using a conductivity dip cell with platinized platinum electrodes. Calibration of the cell will be given by the authors in the companion report.

The amount of fluid in a sample was determined by weighing the sample wet and subtracting its dry weight. Each weighing was determined to within 1 mg on a Mettler balance. A typical sample dry weight was about 100 g and the water adsorbed at full saturation added about 10-12 g. Even after subtraction of the dry from wet weights, the accuracy of measurement was to at least three places.

The desaturation process adopted for the present experiment may have allowed excess free ions to remain in the samples. First, the ions may have diffused more slowly from the samples than did the water; therefore, the ion concentrations in the desaturation "sandwich" may

Table 4.--Estimated percent error of measured resistivity and dielectric constant

[See section Error Analysis, p. 25, for exceptional cases]

Frequency	Estimated resistivity error (percent)	Estimated dielectric constant error (percent)
100 Hz	8	10
1 kHz	8	10
10 kHz	8	25
100 kHz	10	30
1 MHz	10	10
10 MHz	15	10
100 MHz	20	20

not have come to equilibrium in 24 hours. Second, the blotter material had some soluble chloride (Scott and others, 1967). By soaking blotter material in distilled water it was determined that a typical blotter disk contained the equivalent of 20 ohm-meter saturant when fully wetted with distilled water. The effects are additive--both tend to increase the salt concentration and decrease the resistivity of the remaining pore water.

The errors inherent in the measurements of resistivity and dielectric constant as a function of frequency are different for each frequency and for each electrical parameter. The accuracy of measurement listed by the manufacturer of an impedance bridge is for a pure impedance element; for example: a pure capacitance or a pure resistance. When a capacitance and resistance are in parallel and the impedance of one is much lower than that of the other, the stated accuracy applies to the measurement of the lower impedance component only. In the present measurements the capacitive reactance was often two orders of magnitude higher than the shunting resistance of the sample for frequencies at and below 10^5 Hz. On the basis of Wayne Kerr's specifications, the accuracy of the bridges was probably about 1 percent for the resistive component measurements between 100 Hz and 10 kHz and about 3 percent at 100 kHz.

Other factors that affected the accuracy of the resistivity measurement were the blotter electrode impedance and drift of measured values during the time of measurement. Blotter electrode resistances were measured at 1,000 Hz and, in the worst instances, may have been 3 percent

of the sample resistance. Changes of measured parameters (drift) during measurement were occasionally caused by incomplete compression of the blotter electrodes against the sample or, more generally, by electrolyte exchange between blotters and sample. If the drift exceeded 5 percent in one frequency sweep, the measurements were taken over. The measured resistivity typically drifted more than the dielectric constant: 3-4 percent versus 1-3 percent, respectively. On the basis of known errors the estimated accuracy of resistivity measurement at 100 kHz is about 10 percent.

The accuracy of capacitance measurement was affected by lead inductance as well as poor bridge accuracy. The measured low-frequency series capacitance of the blotter electrode system is estimated to be in excess of 0.3 farads in series with earth materials capacitances of not more than 10 microfarads, therefore, the blotter electrode capacitance can be ignored. The best accuracies of dielectric constant measurement were at 100 Hz and 1 kHz (table 4). The measured capacitance at 10 kHz was often so small that only the least two of four significant figures on the capacitance dials of the Wayne-Kerr B221 bridge would register other than zero. The rated accuracy of the bridge is 2.5 parts per thousand on a four significant digit reading. For two digit readings the accuracy ranges between 2.5 and 25 percent for the best and worst cases, respectively. For most readings, the accuracy was about 10 percent; however, table 4 lists the worst case (25 percent).

The capacitance readings at 100 kHz are corrected for the very strong dependence of the capacitive dial setting on the position of the resistance

measuring potentiometer of the Wayne Kerr B601 bridge. A correction curve was generated by measuring the apparent capacitances of a series of deposited carbon resistors at 100 kHz. The resistors have almost no reactive impedance; thus, the capacitance readings represent the corrections for resistive loading, lead inductance, and the reactance of the resistance-measuring potentiometer.

The corrected measured capacitances tend to be higher at 100 kHz than would be predicted by extrapolation from data at other frequencies. Since the tendency is most pronounced when high-resistivity samples are measured, the cause is not bridge loading. Whether the tendency of the data to be higher than expected at 100 kHz is a property of the sample or an artifact of the measurement is unknown.

The probable errors for the resistive and capacitance measurements made on the Hewlett-Packard 250 B R-X bridge at 1, 10, and 100 MHz are difficult to quantify. Judy and Eberle (1969) describe the phosphor bronze band that connects one side of the test cell to a ground and they outline the method by which the sample resistance and capacitance are computed in terms of the series inductance of the band and the measured resistance and capacitance. By an extension of the method of computation, the expected uncertainty of measurement in the computed capacitance of the sample is found to depend on the estimated error of the measured capacitance and that of the measured resistance. The estimated error in computed capacitance can be ten or more times the resistive measurement error if the series inductance and sample capacitance are nearly resonant. Unfortunately, the near-resonance

condition exists at 100 MHz for samples saturated with 0.3 ohm-meter saturants. The computed capacitances of such samples are approximately two to three times their most probable values at 100 MHz.

The uncertainty of computation for the sample resistance is also affected by the near-resonance condition but not as severely as is the uncertainty in the dielectric constant. Also, at 100 MHz, the computed resistances are lower than at the other frequencies, which tends to emphasize errors caused by the inductive band. Therefore, the estimated error in computed resistivity at 100 MHz is larger than that at 1 or 10 MIz.

The tabulated estimates of accuracy are for absolute values and take into account all the foregoing sources of error. When the resistivity data are normalized, as is done in the next section, any sources of error that cause systematically high or low measurement values will cancel; for example, sample-to-sample variations in resistivity. Therefore, the relative accuracies of normalized data can be better than the absolute accuracies listed in table 4.

PREDICTIVE CURVES, DERIVATION

Predictive R- curves

A curve-matching technique for predicting the frequency dependence of resistivity in earth materials was developed from graphs of the resistivity data. Three log-log plots of resistivity versus frequency (figs. 3, 4, and 5) were generated from the resistivity data on fully saturated sandstones, one plot for each kind of sandstone. In addition, similar plots to compare the resistivities of partially and fully saturated

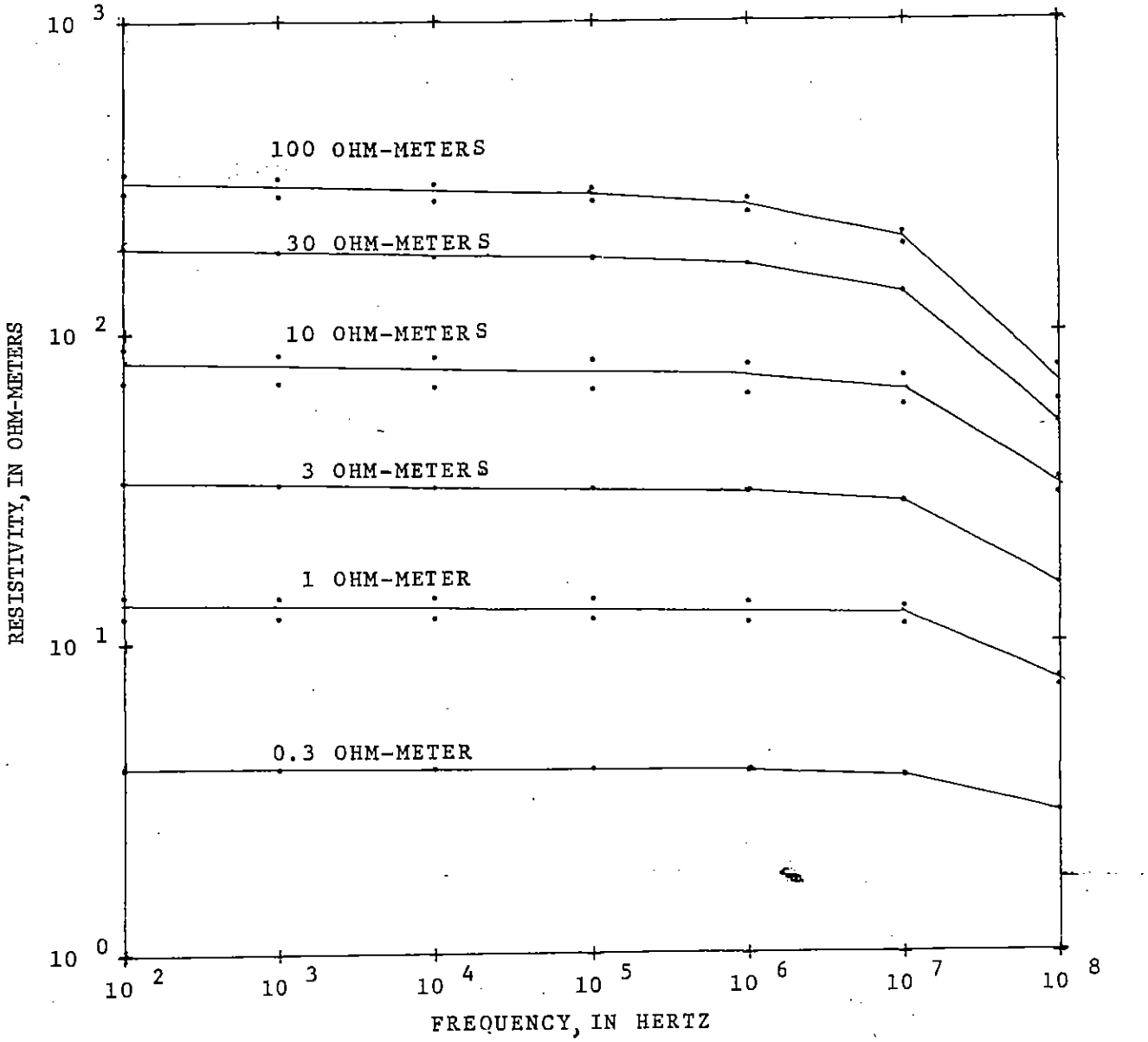

Figure 3.--Resistivity of fully saturated Sunnyside sandstone samples versus frequency. The resistivities of the solutions in which the samples were saturated are indicated next to the curves.

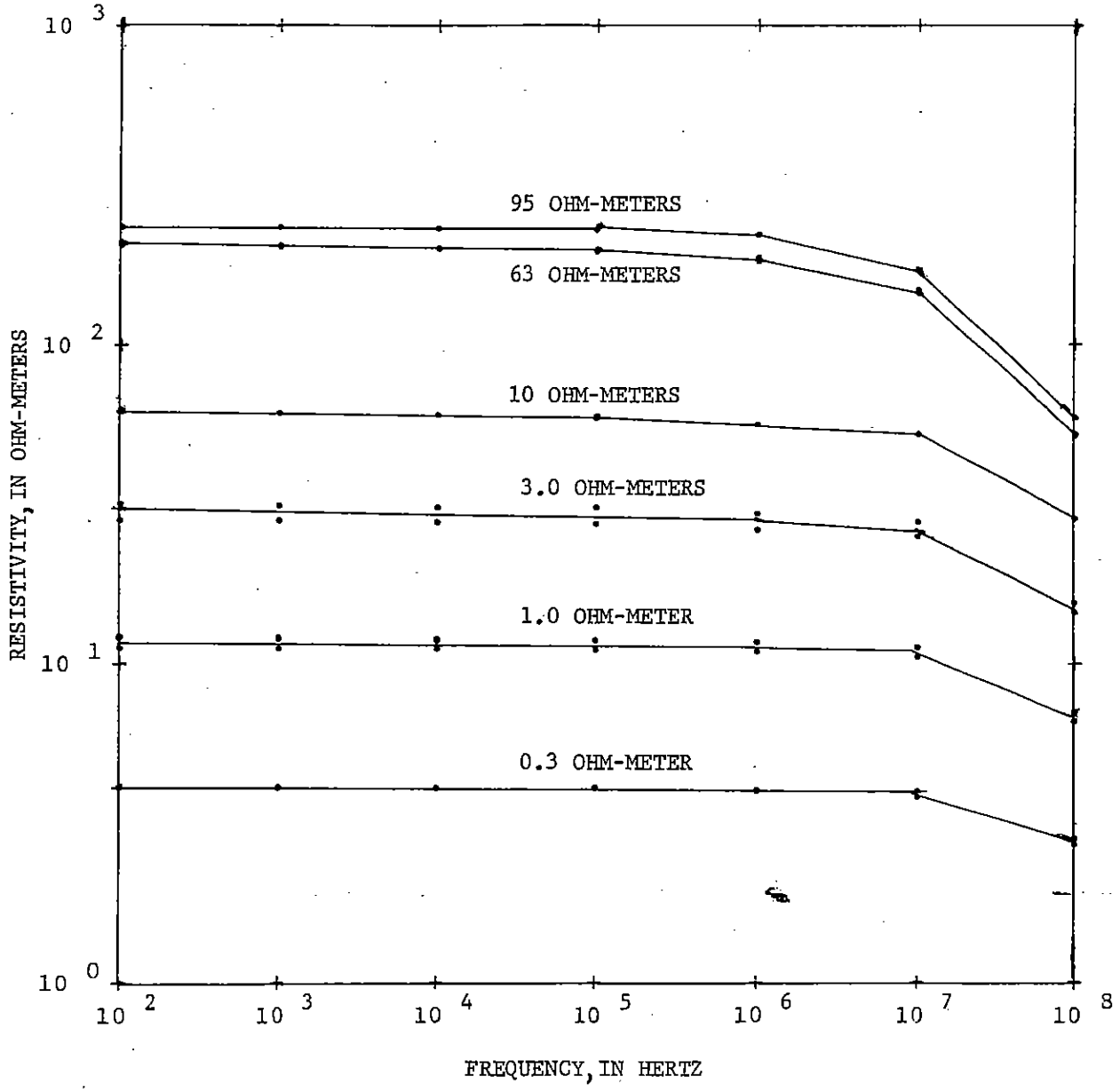

Figure 4.--Resistivity of fully saturated Lyons Sandstone samples versus frequency. Resistivities of the solutions in which the samples were saturated are indicated next to the curves.

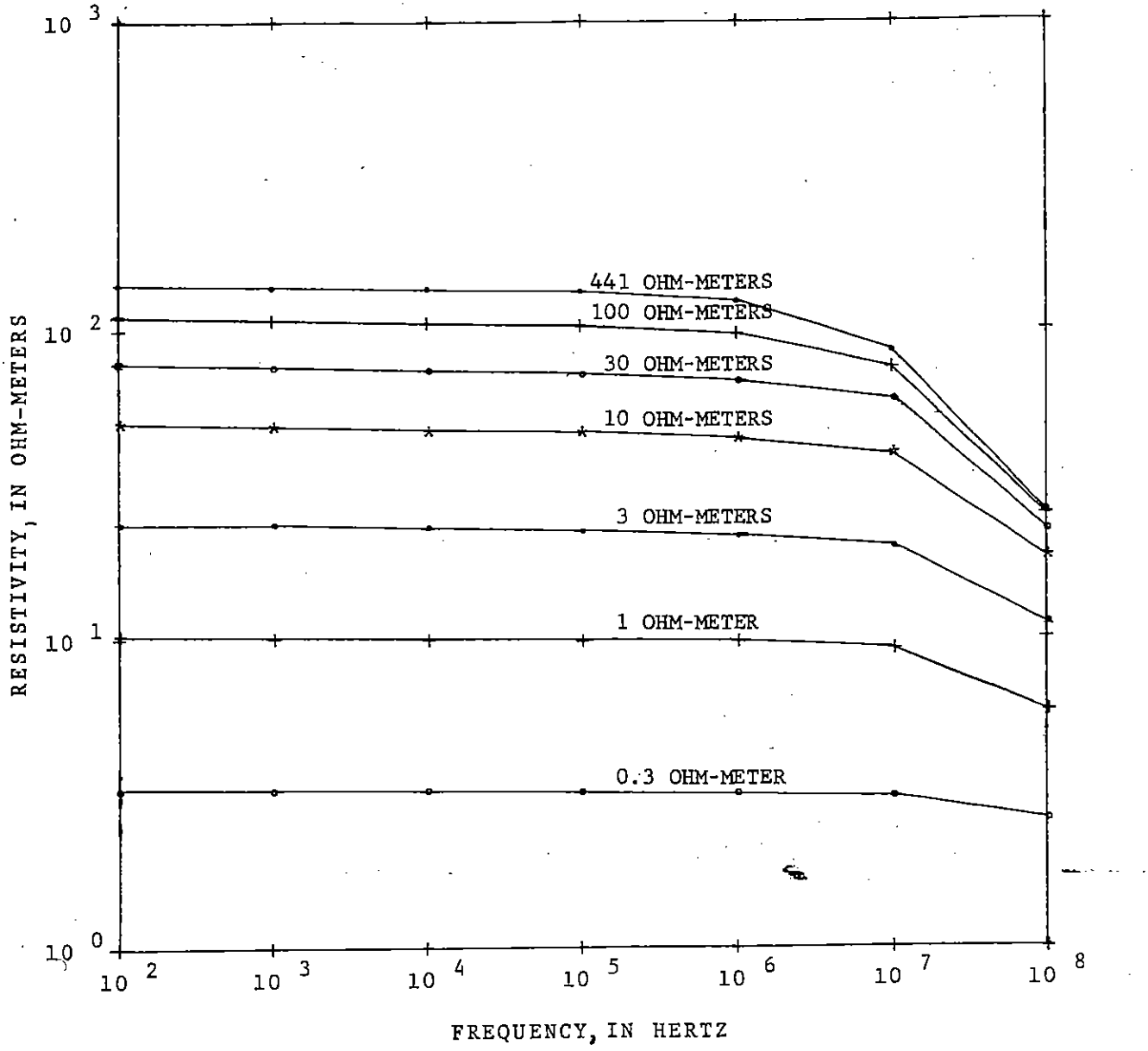

Figure 5.--Resistivity of fully saturated Laramie sandstone samples versus frequency. Resistivities of the solutions in which the samples were saturated are indicated next to the curves.

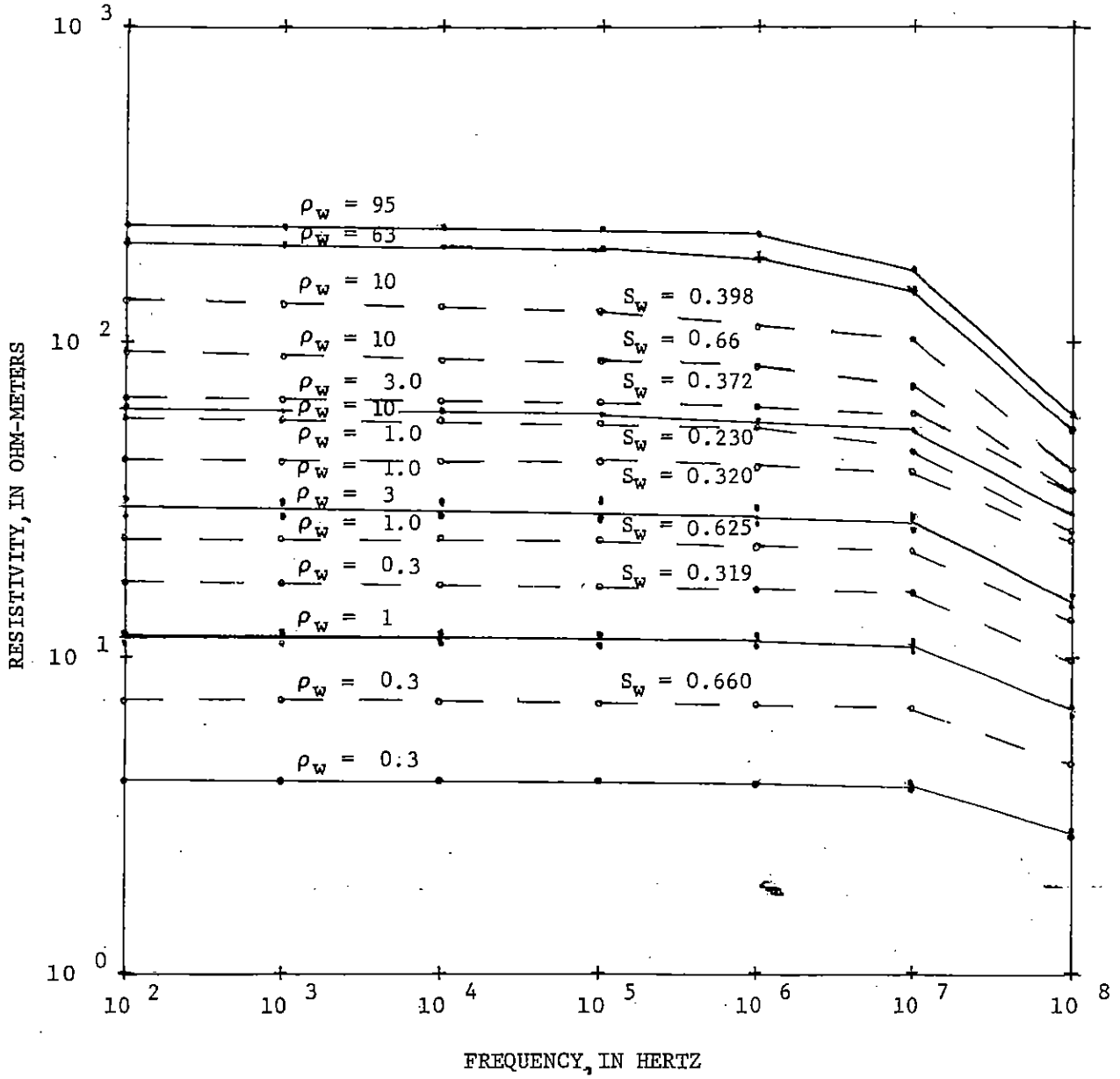

Figure 6.--Resistivity of Lyons Sandstone samples versus frequency. Solid lines indicate fully saturated samples; dashed lines indicate partially saturated samples. The resistivity, ρ_w, of the solution saturating the sample is indicated next to each curve. The fractional water content, S_w, of each partially saturated sample is indicated next to each dashed line curve. The dimensions of ρ_w are ohm-meters.

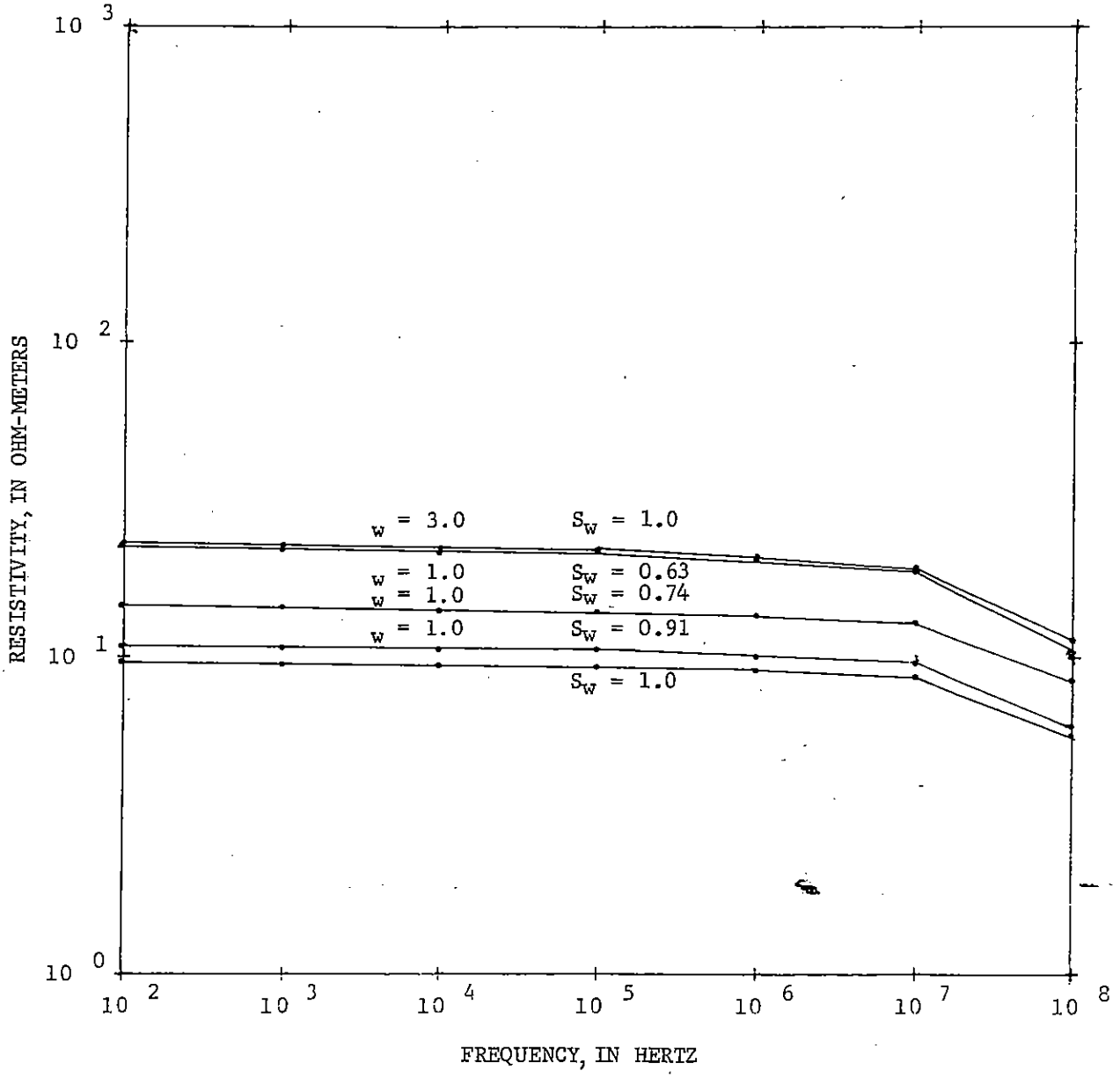

Figure 7.--Resistivity of fully and partially saturated Laramie sandstone samples versus frequency. The resistivities, ρ_w, of the solutions in which the samples were saturated are indicated as are the fractional water contents, S_w, of the samples.

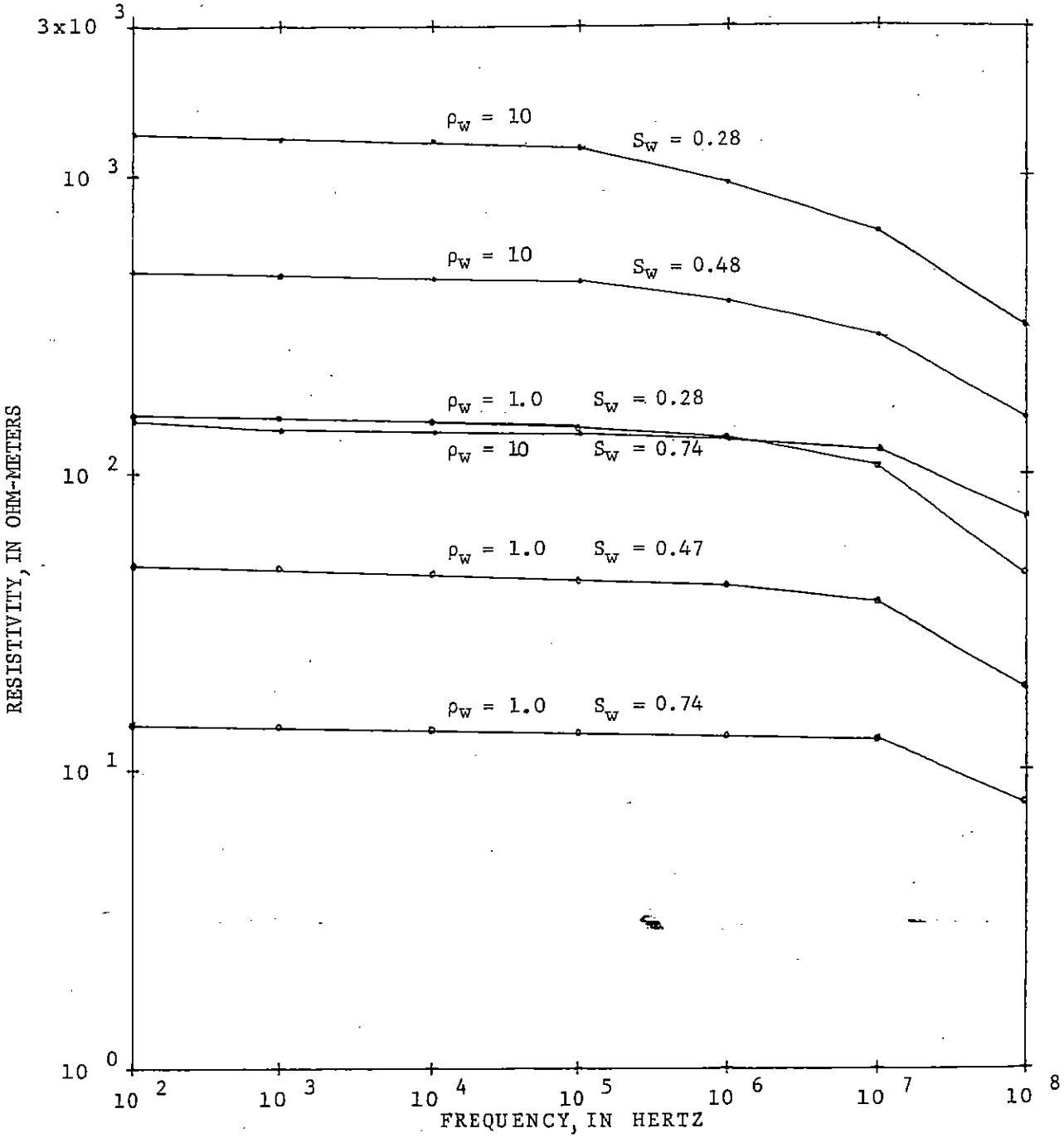

Figure 8.--Resistivity of partially saturated quartz sand mixture having porosity, $\phi = 0.32$, versus frequency. The resistivity, ρ_w, of the solutions in which the samples were saturated and the fractional water content, S_w, are indicated: the dimensions of ρ_w are ohm-meters.

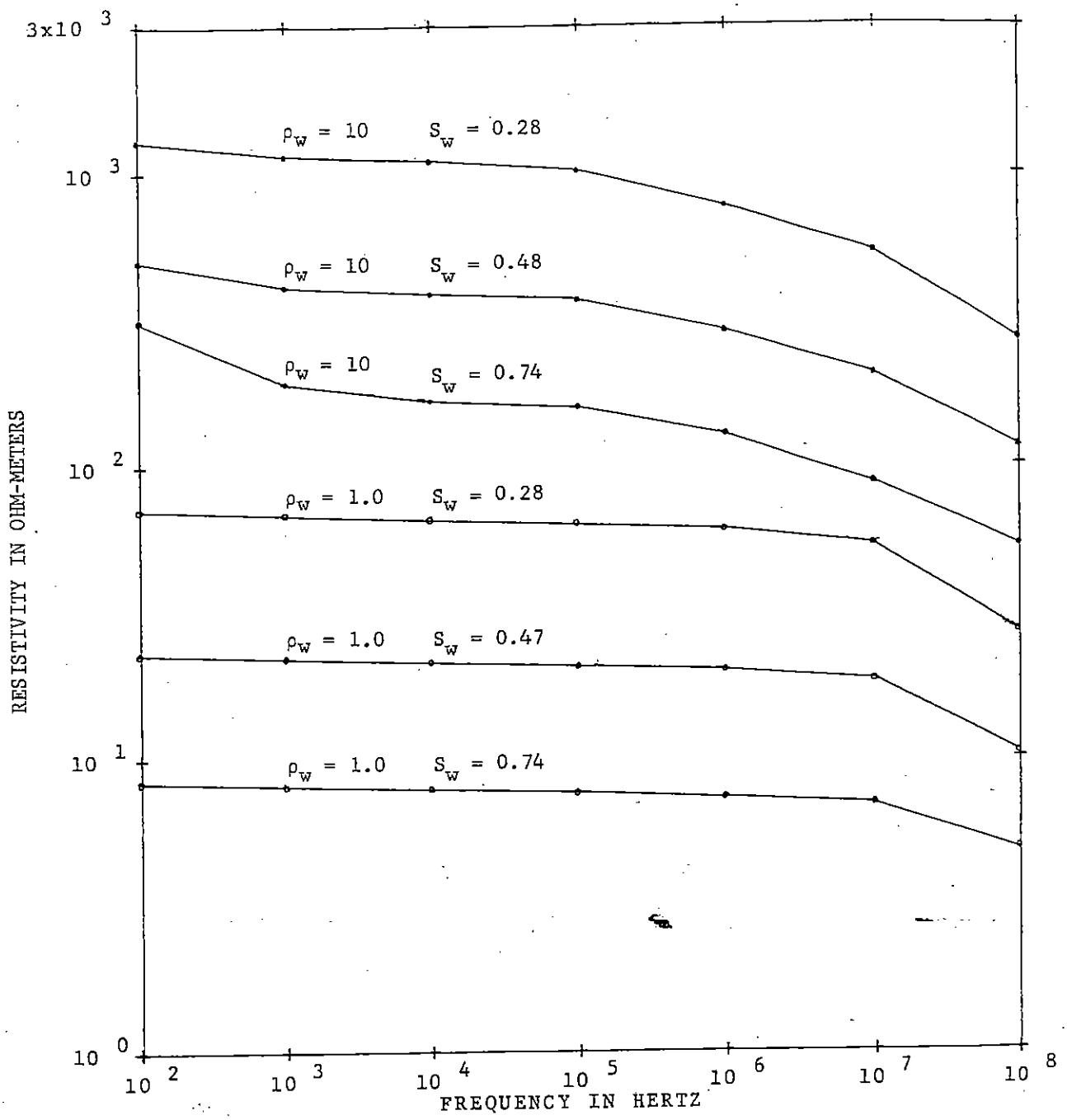

Figure 9.--Resistivity of partially saturated quartz sand mixture having porosity, $\phi = 0.51$, versus frequency. The resistivity, ρ_w, of the solutions in which the samples were saturated and the fractional water content, S_w, are indicated. The dimensions of ρ_w are ohm-meters.

sandstones were generated; for example, figure 6 for Lyons Sandstone and figure 7 for Laramie. The resistivity data from measurements on quartz sands were also plotted (figs. 8 and 9) for comparison with the sandstone curves.

Several features of figures 3, 4, and 5 are notable. Each set of curves forms a well-defined family of curves; the curves trend together and do not cross. Each family is unique in its absolute values of resistivity; for example, the resistivity at 100 Hz of a Laramie sample saturated with 10 ohm-meters water is not the same as that of a Lyons sample with a similar saturant. Within a family of curves, the samples saturated with the lowest resistivity water (ρ_w = 0.3 ohm-meters) show the least frequency dependence; and as the value of ρ_w increases, the dispersion also increases. The latter point suggests that samples from different sandstones might have similarly shaped resistivity dispersion curves if the resistivity of the saturating water for each sample is the same. Because the resistivity data are plotted on a logarithmic scale, superposing the curves is equivalent to normalizing them. When curves for correspondingly saturated samples are superposed, the shapes of the curves are found to closely match for any two or more sandstones saturated with water of the same resistivity. The curves match much better than the absolute errors listed in table 4 suggest; the plotted points scatter no more than 5 percent from the median for frequencies at and below 10 MHz and no more than 10 percent at 100 MHz. The matching of curves for different types of sandstones is the basis on which the set of predictive curves for resistivity as a function of frequency is developed.

Each set of resistivity data for saturated sandstones was normalized by letting the resistivity at 100 Hz equal 1 then the sets of data were collected into groups using ρ_w as a parameter. Six empirical curves were plotted in figures 10-15 using the groups of normalized resistivity data for ρ_w = 0.3, 1.0, 3.0, 10, 30 and 100 ohm-meters, respectively. These plots, called the R-curves, are the predictive curves for resistivity as a function of frequency; they are collected together at the end of the text (p. 52). Because each normalized resistivity curve is associated with one value of ρ_w, it is convenient to label each curve by a parameter, called R_w, which is equal in the value to the ρ_w associated with the curve. For previously given reasons, the matrix material is considered to be secondary in determining the electrical properties of earth materials; therefore, the normalized resistivity curves should predict the frequency dependence of earth materials other than the sandstones.

The predictive R-curves yield values of resistivity at frequencies between 100 Hz and 100 MHz that are relative to the value of resistivity of 100 Hz. Thus, to use the curves, one measured value of resistivity must be known for the material. Since the resistivity of a typical earth material is almost constant for frequencies $\leq$100 Hz; resistivity values that are measured in situ at low frequencies can be used as approximations of the 100 Hz values.

The predictive curves are derived from the measurements on fully saturated sandstones that have porosities in the range ϕ = 0.209 to ϕ = 0.255; therefore, it remains to be shown that the curves can be applied to partially saturated earth materials or to materials with

other porosities. If the resistivities of partially saturated samples are plotted as a function of frequency, as in figure 6, the plots are found, within experimental error, to fall in the same family of curves as those of fully saturated sandstones. The Lyons Sandstone data, shown in figure 6, are an extreme example since the fractional water content varies over a range of more than four to one: $0.23 \leq S_w \leq 1.0$.

The observation that dispersion curves for fully and partially saturated sandstone fall in the same family of curves for each material implies that materials with identical low-frequency resistivities have identical resistivity dispersion curves. Thus, the R-curves, derived from the resistivities of fully saturated materials, should be applicable to the dispersion of resistivity in partially saturated materials, provided a method of finding the correct curve is available.

The following formula can be used to find the appropriate R_w curve for a partially saturated material:

$$R_w = \frac{\rho_w \rho_t}{\rho}$$

where as previously ρ_t is the resistivity at low frequencies (≤ 100 H_z) of the partially saturated material, ρ is the low-frequency resistivity of the same material when fully saturated, and ρ_w is the resistivity of the saturating water. The R-curve designated by the value of R_w that is closest to the computed R_w is used to predict the frequency dependence of the partially saturated sample.

Two simplifying assumptions are made in deriving the formula. First, all the dispersion curves of a given material fall in the same family of curves; second, the value of m in Archie's law is strictly constant and does not depend on ρ_w.

the two kinds of material. This observation is consonant with the conclusion reached by Scott, Carroll, and Cunningham (1967) that water content is the primary factor in determining dispersion.

The foregoing considerations suggested that an empirical equation relating R_w, ρ_w, and the water content ($S_w \phi$) could be devised. The empirical equation

$$R_w = 0.18\ \rho_w (S_w \phi)^{-2}$$

predicts the best match between the R-curves and the dispersion curves of the quartz-sand mixtures saturated with 1.0 ohm-meter saline solutions. The predicted value of R_w from the equation is within 30 percent of the nominal value of R_w that labels the matching R-curve.

The frequency dependence of the resistivity of the quartz sands containing 10-ohm-meter solutions is poorly predicted because the shapes of those dispersion curves are different from the R-curves. The shapes of some of the 10-ohm-meter curves in figures 8 and 9 indicate an increasing resistivity with decreasing frequency below 1 kHz. The increase is probably caused by polarization at the electrodes as a discussion in Scott, Carroll, and Cunningham (1967) indicates. The shape of the curves at frequencies above 10 kHz also disagrees with the closest matching R-curves. In the worst instances, the actual resistivities of the quartz sands are about 30 percent below the predicted values at 1 MHz and about 50 percent below at 10 and 100 MHz.

It is hypothesized that the differences between actual and predicted resistivity values not attributable to electrode polarization are caused by the presence of clay in the sandstones and its absence in the quartz

sands. As the R-curves are constructed from the sandstone data, they reflect the effects of clay content. As is mentioned in the Theoretical Background section, the presence of clay strongly affects the bulk resistivity at low frequencies of an earth material if the pore water is very fresh; this is the origin of the ρ_{limit} term in Wyllie's (1963) extension of Archie's law.

The curve comparisons given above indicate that for saturants with resistivities near 1.0 ohm-meter, clay content is secondary in determining frequency dependence of resistivity in earth materials; however, for saturants with resistivities of 10 or more ohm-meters, the presence or absence of clay affects the dispersion characteristics to the extent noted above.

Dielectric constant predictive curves

The fact that dielectric constants of earth materials are rarely measured in the field precludes using a normalized curve method, similar to the R-curves, for prediction of dielectric constant as a function of frequency. Two other approaches are employed instead. First, the relationships between the real and imaginary parts of the dielectric constant are used to construct a set of κ versus $(2\pi f \epsilon_o \rho)^{-1}$ curves (figs. 16-19); second, a pair of curves is generated for predicting the dielectric constant at 100 MHz (fig. 20).

As indicated in the Theoretical Background section (p. 6) the relaxation-time theory ties together the resistivity and dielectric constant of earth materials by defining a complex dielectric constant

$$\kappa = \kappa + j\kappa''$$

where κ is the usual dielectric constant, $j=\sqrt{-1}$, and κ'' is defined by

$$\kappa'' = (2\pi f \varepsilon_o \rho)^{-1}$$

The data in this study do not extend to sufficiently low frequencies to use the usual Cole-Cole plot analysis (see, for example, Arulanandan and Mitchell, 1968); however, some correlations between ρ and κ that are observed in the data suggest that κ and κ'' are the appropriate variables with which to relate ρ to κ. First, the dielectric constant is highest for the lowest resistivity samples and vice versa. Second, the resistivity is approximately a constant over the range of frequencies in which the dielectric constant decreases as approximately inverse frequency. Because κ'' is proportional to inverse resistivity, high values of κ are associated with high values of κ'' and low values of κ with low values of κ''. Where ρ is a constant, κ'' decreases as inverse frequency. Therefore, in the frequency range 100 Hz to approximately 100 kHz, in which both the above-mentioned conditions approximately hold, a plot of κ versus κ'' should be a nearly straight line.

The data in the appendix were grouped together by value of ρ_w and were used to plot figures 16-19. The approximately straight-line portion of each plot is nearly independent of frequency, the type of sandstone, the value of S_w, and the porosity. The latter point was demonstrated by plotting measured quartz-sand dispersion data on figures 16 and 18. After eliminating polarization effects, the quartz-sand data plot as closely to the ρ_w = 1.0 and $\rho_w = \geq 10$ ohm-meters curves as the sandstone data.

The straight-line portions of the curves in figures 16-19 are nearly parallel but are displaced from each other; thus, the ratio of κ to κ'' depends on ρ_w. When the curves are constructed from data for which $\rho_w \geq 10$ ohm-meters the curves overlap; for this reason all the $\rho_w \geq 10$ ohm-meters data are plotted together in figure 16.

At frequencies above 1 MHz, the dielectric constant is not dominated by ionic effects as it is below that frequency. The evidence in Bondarenko (1965), for instance, shows that the dielectric constant of a dry earth material is no less than half of the dielectric constant of the same material when wet. As was pointed out in the Introduction, the dielectric constant approaches a limiting value at frequencies in excess of 1 MHz. The limiting value of the dielectric constant depends on the porosity and fractional water content of the material as well as on the material itself.

Because κ'' is proportional to inverse frequency, the limiting values for κ in figures 16-19 are approached at small κ'' values. The plots of κ versus κ'' diverge in the megahertz frequency range into a family of curves. The maximum divergence is at 100 MHz where the curves closely approach their limiting values. Three members of each family of curves are shown on figures 16-19, to illustrate the range of variation.

To find the appropriate κ versus κ'' curve for a particular material, the limiting value of dielectric constant, or the value at 100 MHz, is needed. An empirical method, , for predicting the dielectric constant at 100 MHz is developed using the experimental data in the Appendix.

Von Hippel (1954) quotes a logarithmic mixing formula to relate dielectric constant at 100 MHz to water content and porosity for the quartz-sand mixtures. In the notation of the present paper,

$$\ln \kappa = (1-\phi) \ln \kappa_m + (S_w\phi) \ln \kappa_w$$

where κ_m and κ_w are the matrix and water contributions to the dielectric constant respectively.

The multipliers of the logarithms in each case are the fractional volumes occupied by each material. The equation can be rearranged into a more convenient form by dividing through by $(1-\phi)$

$$\left(\frac{1}{1-\phi}\right) \ln \kappa = \ln \kappa_m + \frac{(S_w\phi)}{(1-\phi)} \ln \kappa_w$$

In this equation the quantities $(S_w\phi)$ and $(1-\phi)$ are assumed to be known. The quantity κ_m is unknown but generally has values between 4 and 6 for common earth materials. The quantity $\left(\frac{1}{1-\phi}\right) \ln \kappa$ is plotted as a function of $\frac{(S_w\phi)}{(1-\phi)}$ in figure 20. If the mixing formula is valid and κ_m is approximately a constant, the plots are straight lines with slopes of $\ln \kappa_w$ and intercepts on the y-axis of $\ln \kappa_m$. The κ_w term includes the dielectric constant of the water and the contributions to the dielectric constant of free ions and of ions interacting with clay particles; therefore, the term can have values greater than the dielectric constant of water at 100 MHz.

All the dielectric constant data at 100 MHz for materials containing ρ_w = 1.0-ohm-meter water are plotted in figure 20 and the best straight-line fit is shown; also plotted is the best straight-line fit to the dielectric constant data at 100 MHz for materials containing $\rho_w \geq$10-ohm-

meter water. Both lines intercept the y-axis at values for κ_m between 4 and 6; the crossing of the lines is probably not statistically significant.

The mixing formula method does not consider earth material resistivity; thus, it works best at 100 MHz where the dielectric constant least depends on resistivity. The method was tried at lower frequencies using the experimental data and was poorly predictive of dielectric constant compared to the κ versus κ'' curves. However, the mixing formula method may be applicable at frequencies in excess of 100 MHz if the dielectric constant continues to be asymptotic to a constant at those frequencies.

INSTRUCTIONS FOR USING THE PREDICTIVE CURVES

In this section, the instructions for using the predictive curves are collected and the estimated limits of accuracy of prediction are given.

Predictive R-curves

To use the R-curves to predict the dispersion of resistivity in an earth material the following information is needed. A low-frequency ($\leq$100 Hz) value for the resistivity of the earth material must be measured either in situ or in the laboratory, and the resistivity of the water that invades the material, such as well water, must be known. In some instances either the porosity ϕ and the water contents ($S_w\phi$) or the low-frequency ratio of the resistivity of the material to the resistivity of the same material fully saturated (ρ_t/ρ) must be known or estimated.

Each R-curve is labeled by a parameter R_w. To select a resistivity dispersion curve for an earth material, an approximate value of R_w must be computed in one of the following ways:

(a) if $0.15 \leq \emptyset \leq 0.30$ and the material is fully saturated, set $R_w = \rho_w$ to determine the correct R-curve.

(b) if $0.15 \leq \emptyset \leq 0.30$ and the material is partially saturated, set $R_w = \rho_w \frac{\rho_t}{\rho}$ to determine the correct R-curve. If preferred, Archie's desaturation equation $\rho_t/\rho = (S_w)^{-n}$ may be used in the equation.

(c) if $\emptyset$ is not in the interval between 0.15 and 0.30 the equation $R_w = 0.18\ \rho_w\ (S_w\emptyset)^{-2}$ is used to determine the appropriate R-curve. The foregoing three methods will estimate to within one R-curve of the optimum dispersion curve according to present experience. Once the R-curve is found for a material, the resistivity of the material at any frequency can be determined by multiplying the normalized resistivity, read from the curve at that frequency, by the value of ρ_o for the material.

Experience indicates that the relative dispersion of materials with $\rho_w \leq 3$ ohm-meters will be predicted within 10 percent between 100 Hz and 10 MHz and within 20 percent at 100 MHz.

For clay-containing materials, in which ρ_w is ≥ 10 ohm-meters, the estimated accuracy of the relative dispersion curves is within 10 percent between 100 Hz and 1 MHz, 20 percent at 10 MHz, and 30 percent at 100 MHz. For clay-free materials with $\rho_w \geq 10$ ohm-meters, the predictive curves will overestimate the resistivity by as much as 30 percent at 1 MHz and 50 percent at 10 and 100 MHz.

Dielectric constant predictive curves

The dielectric constant, κ, can be predicted at any frequency, f, between 100 Hz and 100 MHz if the resistivity of the material is known at the same frequency. The predictive curves for dielectric constant are

the κ versus κ'' curves (figs. 16-19) and the logarithmic mixing formula curves (fig. 20) located at the end of the text. The quantity $\kappa'' = (2\pi f\ \varepsilon_o \rho)^{-1}$, where $\varepsilon_o = 8.854 \times 10^{-12}$ farad/meter, must first be computed. The known value of ρ_w for the water in the material determines which of figures 16-19 is to be used. If ρ_w is greater than or equal to 10 ohm-meters, use figure 16. Find the computed value of κ'' on the horizontal axis of the figure, read vertically to the curve then horizontally to the left vertical axis to find the dielectric constant κ at the specified frequency.

Each κ versus κ'' plot diverges into a family of curves at frequencies in excess of 1 MHz; the divergence is greatest at 100 MHz. If greater accuracy of predicition is needed for dielectric constant at 100 MHz than is obtainable from the κ versus κ'' curves alone, the plots in figure 20 can be used.

The dielectric constant at 100 MHz can be estimated from figure 20 if the water content ($S_w\phi$) and the quantity ($1-\phi$) are known. To use figure 20, compute $(S_w\phi)\ (1-\phi)^{-1}$ and locate the computed value on the horizontal axis of the figure. Determine which of the two curves in figure 20 best approximates ρ_w for the earth material in question, read vertically to that curve from the computed value of $(S_w\phi)\ (1-\phi)^{-1}$, and then read horizontally to find $[(1-\phi)^{-1} \ln \kappa]$. If the reading is denoted by y,

$$y = (1-\phi)^{-1} \ln \kappa$$

then

$$\kappa = \exp\ (y/(1-\phi))$$

yields the computed value for κ at 100 MHz.

The computed value of κ at 100 MHz can be used to estimate κ at frequencies between 1 and 100 MHz. On each κ versus κ'' curve, there is drawn a short straight-line segment through the 100 MHz data. Locate the computed κ at 100 MHz on that line then find the nearest member of the κ versus κ'' family of curves that intersects the line; this member is the best predictive curve for κ at all frequencies.

The estimated uncertainty in the prediction of dielectric constant is about 30 percent provided the best member curve is used and the resistivity of the material is perfectly known. The uncertainty in the resistivity of the earth material should be added to that of the dielectric constant to determine the total uncertainty in the determination of κ. The estimated error in determining κ from figure 20 is about 20 percent.

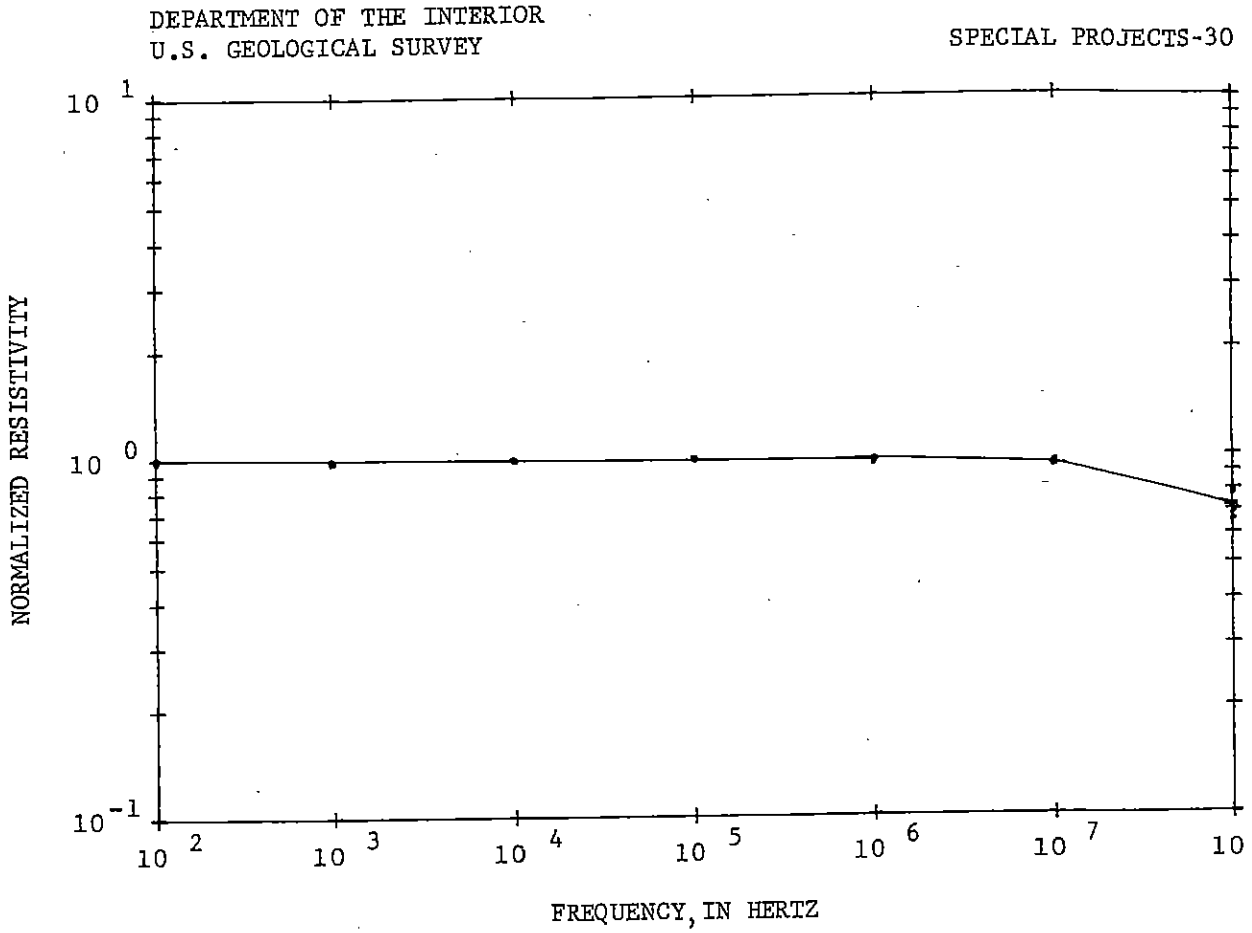

Figure 10.--Predictive R-curve; R_w = 0.3. See pages 48-49 for instructions on the use of the curve.

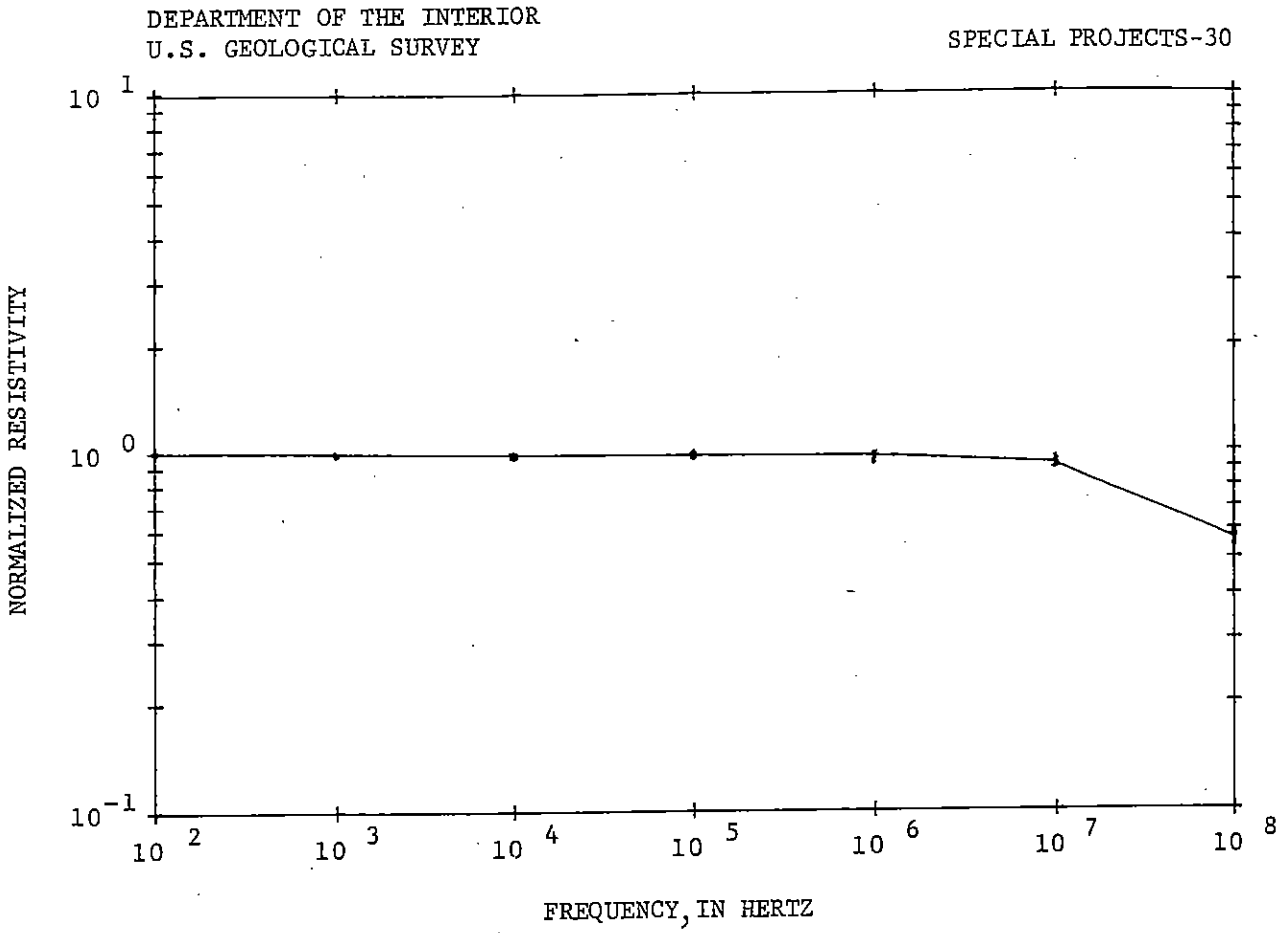

Figure 11.--Predictive R-curve R_w = 1.0. See pages 48-49 for instructions on the use of the curve.

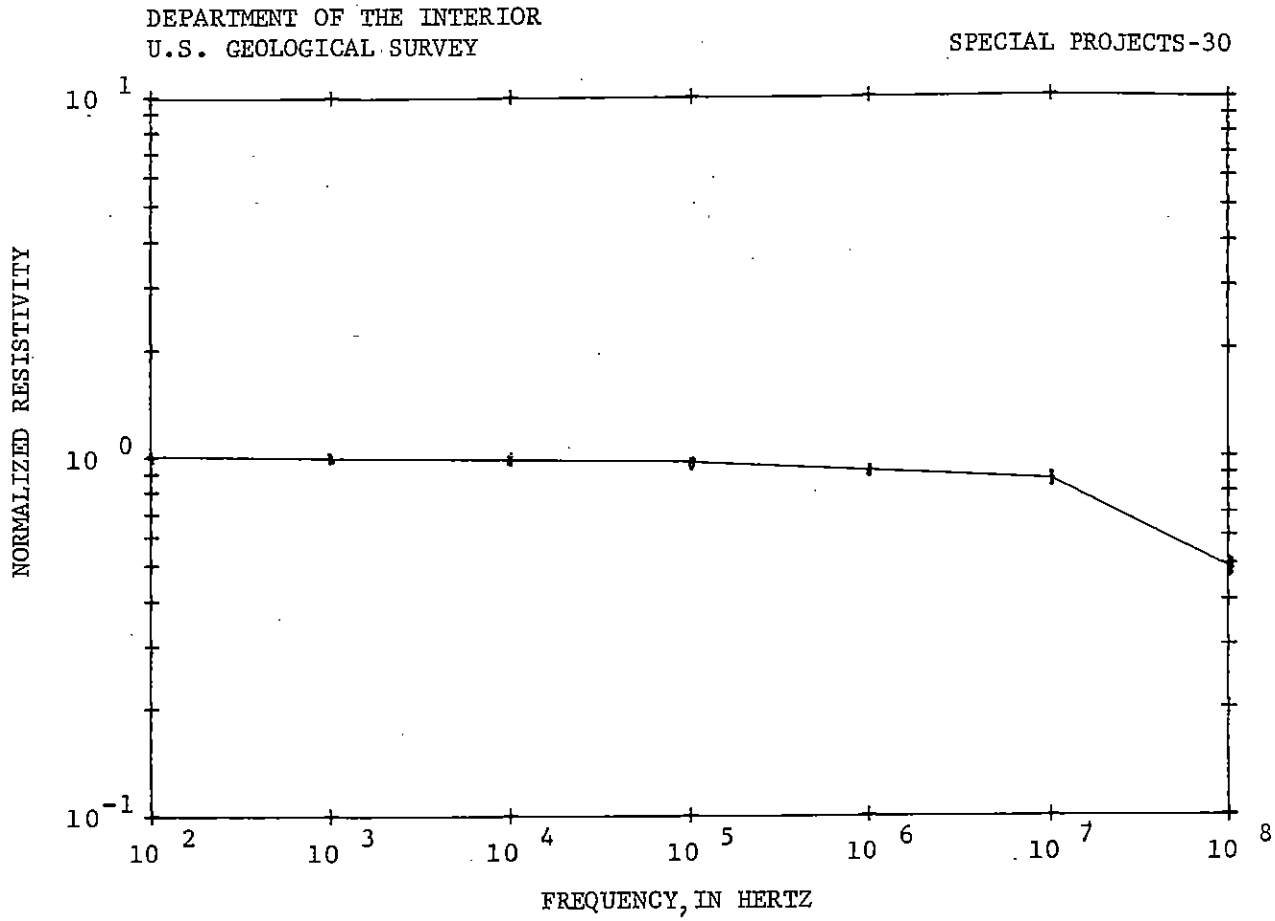

Figure 12.--Predictive R-curve R_w = 3.0. See pages 48-49 for instructions on the use of the curve.

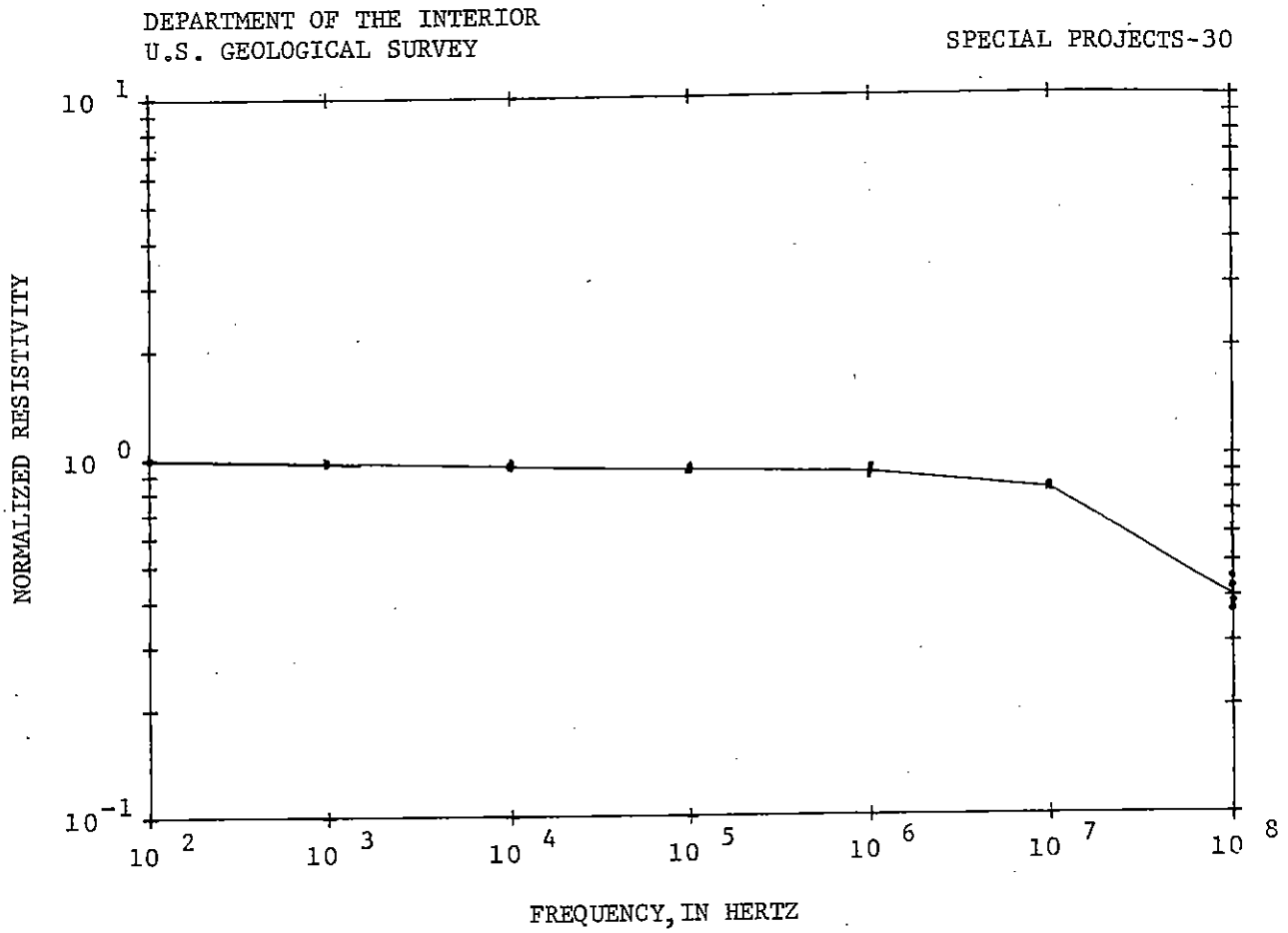

Figure 13.--Predictive R-curve R_w = 10. See pages 48-49 for instructions on the use of the curve.

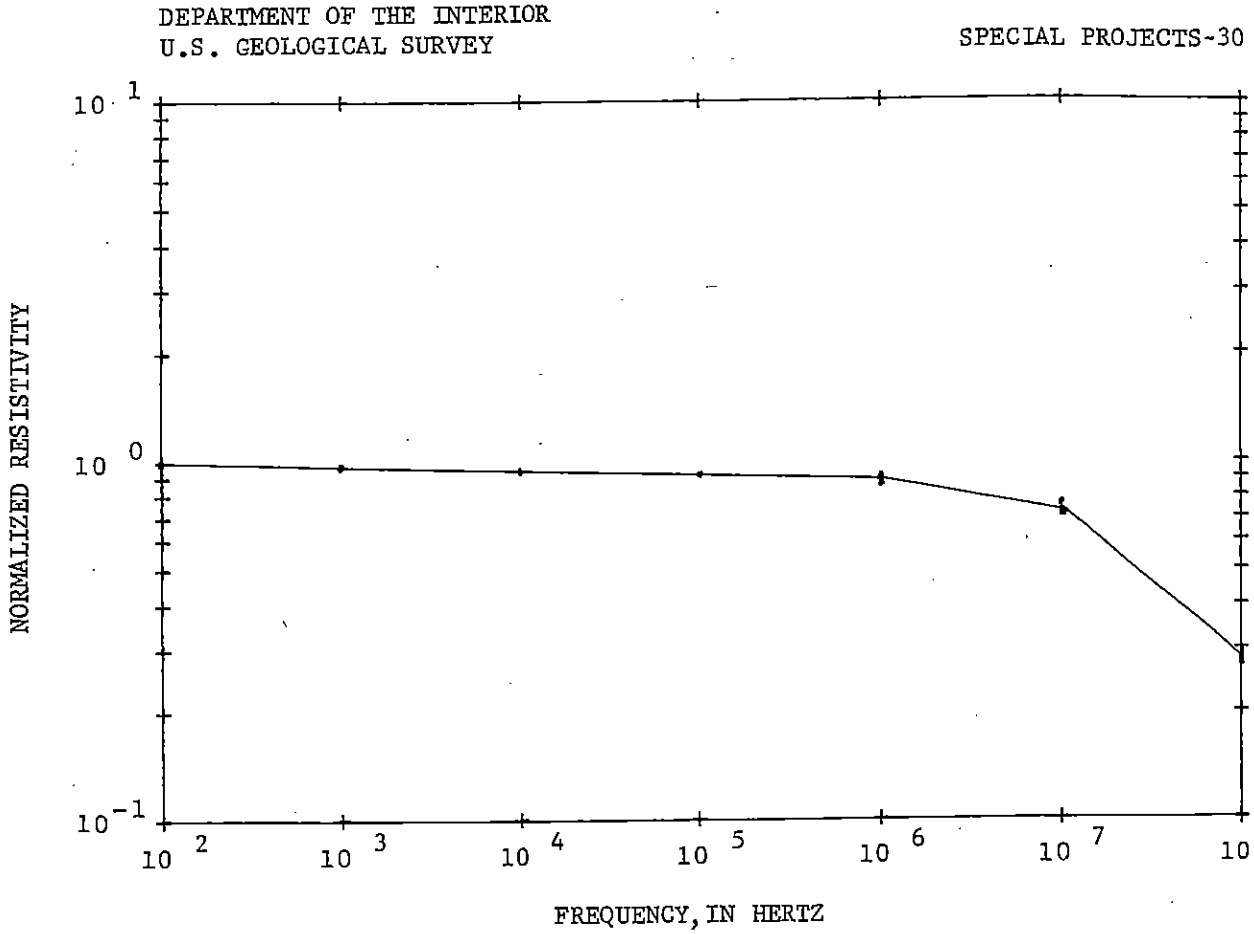

Figure 14.--Predictive R-curve R_w = 30. See pages 48-49 for instructions on the use of the curve.

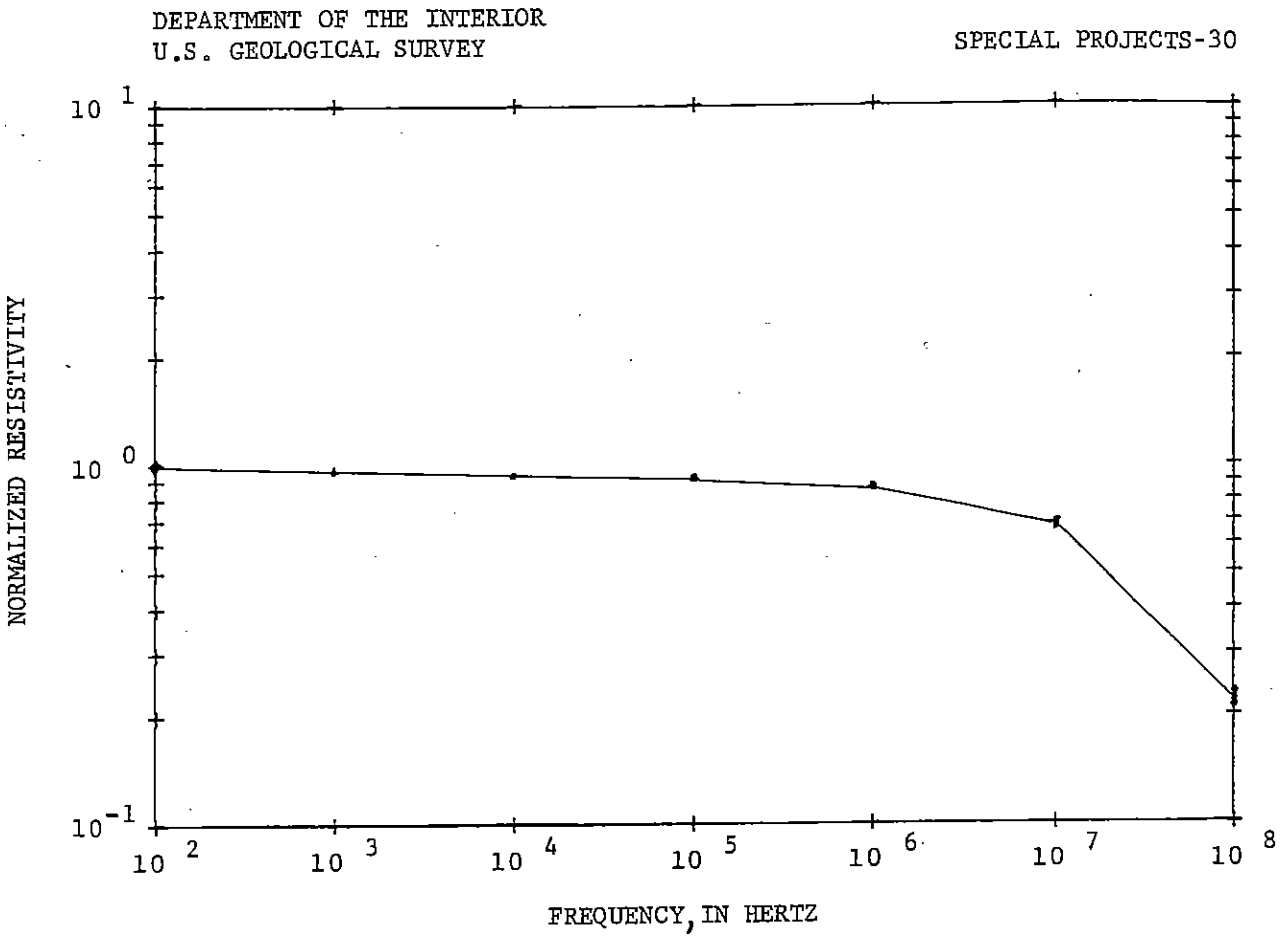

Figure 15.--Predictive R-curve R_w = 100. See pages 48-49 for instructions on the use of the curve.

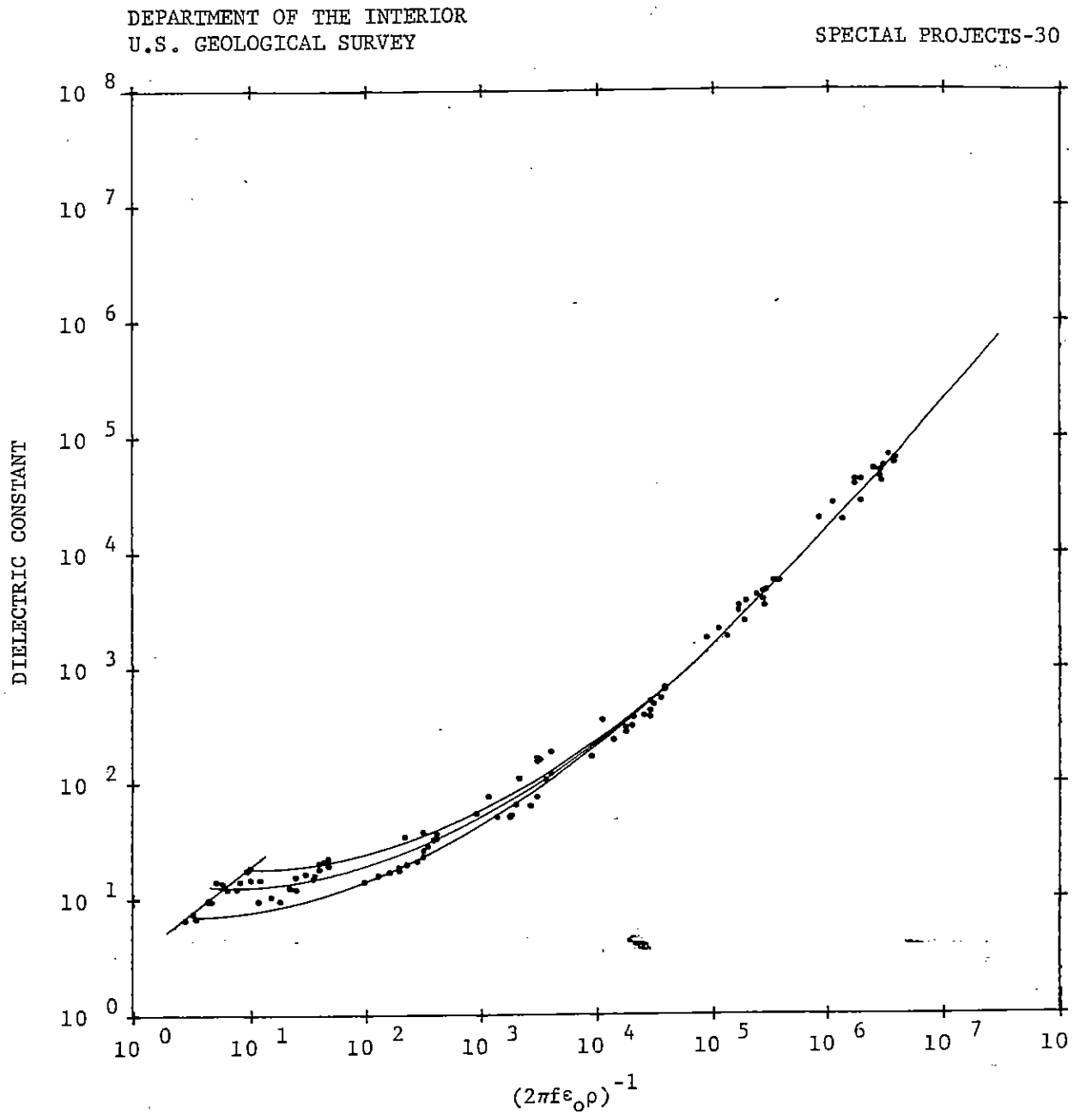

Figure 16.--Predictive curve: κ versus $\kappa'' = (2\pi f\varepsilon_o\rho)^{-1}$. All data for materials with saturant resistivities $\rho_w \geq 10$ ohm-meters. Instructions on the use of this curve are given on pages 49-51.

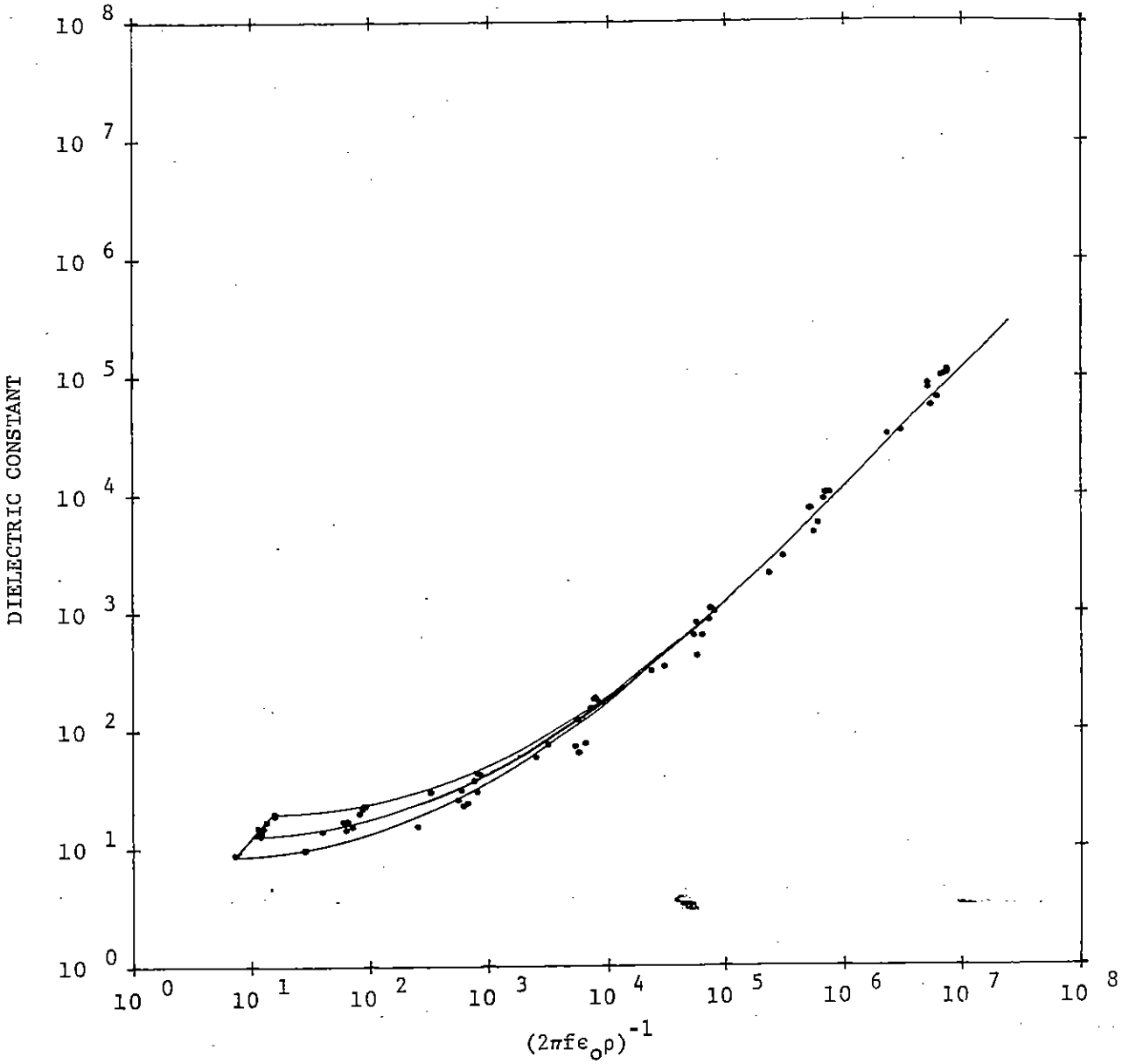

Figure 17.--Predictive curve: κ versus $\kappa'' = (2\pi f\epsilon_o\rho)^{-1}$. All data for materials with saturant resistivity ρ_w = 3.0 ohm-meters. Instructions on the use of this curve are given on pages 49-51.

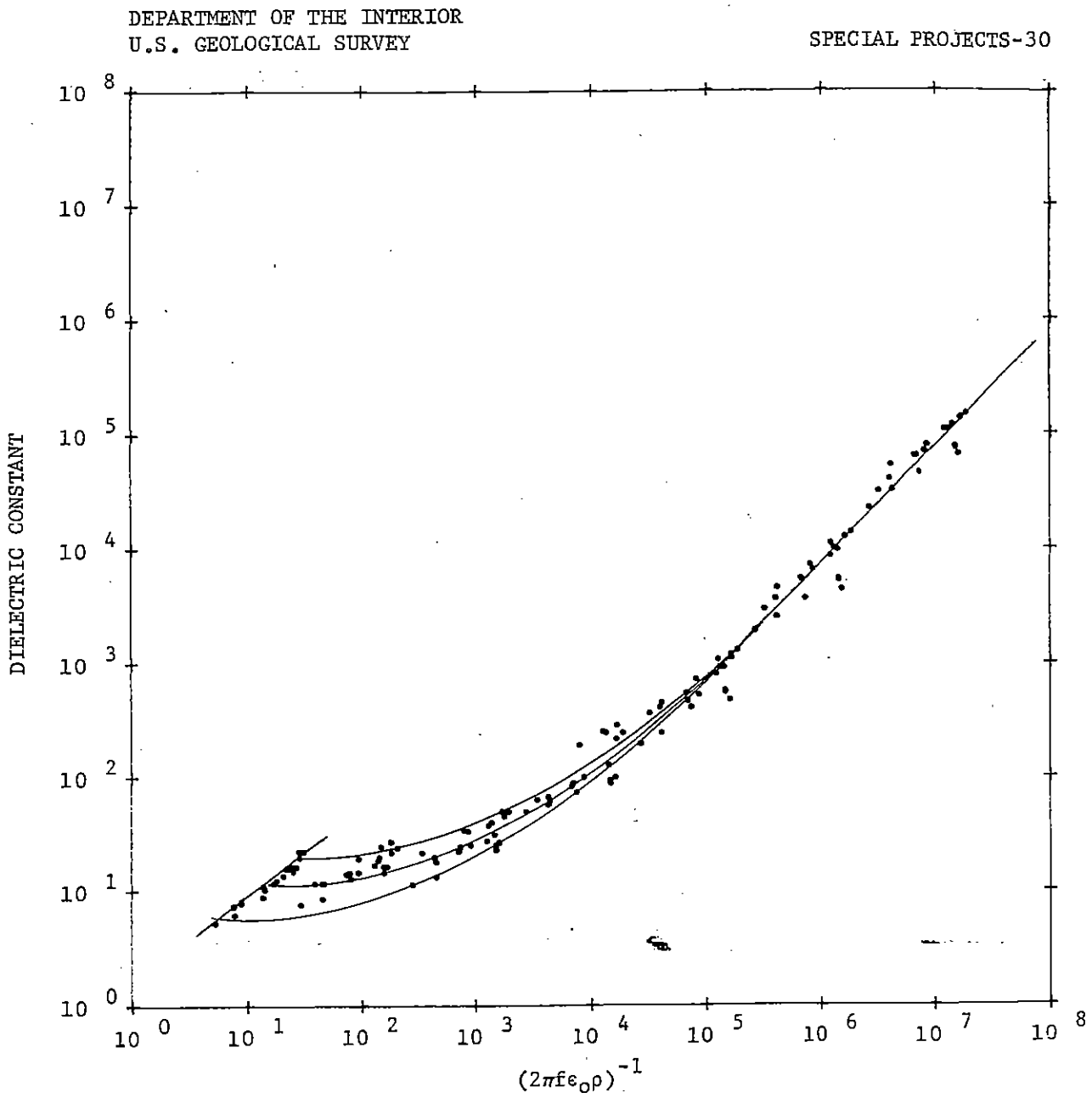

Figure 18.--Predictive curve: κ versus $\kappa'' = (2\pi f\epsilon_o\rho)^{-1}$. All data for materials with saturant resistivity ρ_w = 1.0 ohm-meters. Instructions on the use of this curve are given on pages 49-51.

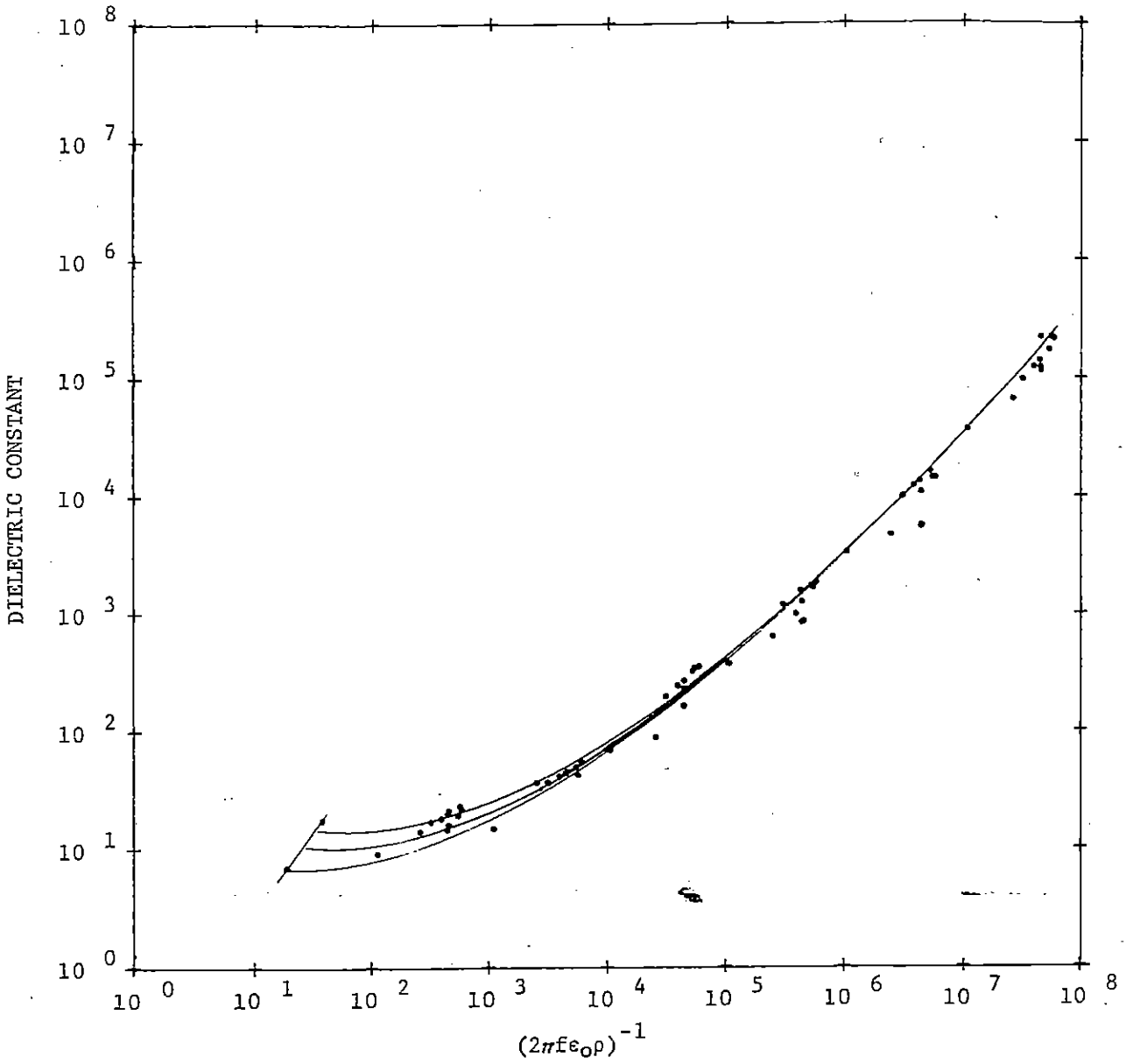

Figure 19.--Predictive curve: κ versus $\kappa'' = (2\pi f\epsilon_o\rho)^{-1}$. All data for materials with saturant resistivity ρ_w = 0.3 ohm-meters; data at 100 MHz are extrapolated (see text, p. 29). Instructions on the use of this curve are given on pages 49-51.

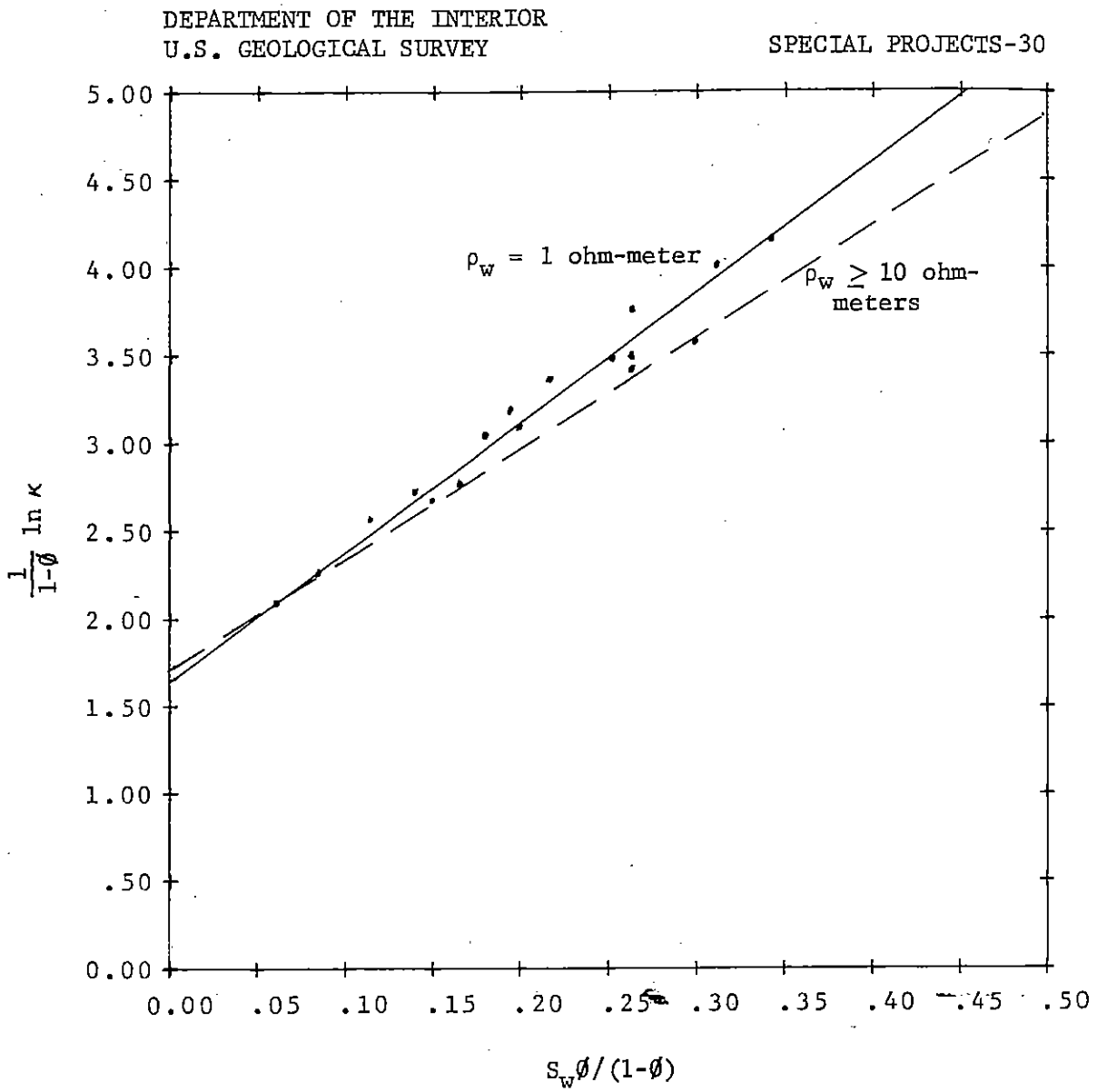

Figure 20.--Predictive curve for κ at 100 MHz; $\frac{1}{1-\phi} \ln \kappa$ versus $S_w\phi/(1-\phi)$. Data from sandstones that contain ρ_w = 1.0 ohm-meter are plotted. Solid curve is for samples that contain ρ_w = 1.0-ohm-meter water; dotted curve is for samples that contain $\rho_w \geq$10-ohm-meter water.

REFERENCES CITED

Alger, R. P., 1966, Interpretation of electric logs in fresh water wells in unconsolidated formations, in SPWLA Logging Symposium, 7th Ann., Tulsa, Okla., 1966, Trans.: Houston, Tex., Soc. Prof. Well Log Analysts. P. CC1-CC25.

Archie, G. E., 1942, The electric resistivity log as an aid in determining some reservoir characteristics: Am. Inst. Mining Metall. Engineers Trans., v. 146, p. 54-62.

Arulanandan, Kandiah, and Mitchell, J. K., 1968, Low frequency dielectric dispersion of clay-water-electrolyte systems: Clays and Clay Minerals, v. 16, no. 5, p. 337-351.

Bondarnecko, A. T., 1965, The frequency dependence of dielectric properties of rock from the Kola peninsula: Physics of the Solid Earth, no. 5, p. 350-354.

Emerson, D. W., 1969, Laboratory electrical resistivity measurements of rocks: Australian Inst. Mining and Metallurgy Proc., no. 230, p. 51-62.

Fuller, B. D., and Ward, S. H., 1969, Linear system description of the electrical parameters of rocks: Inst. Elec. Electronic Engineers Trans. Geosci. Electronics, v. GE-8, no. 1, p. 7-18.

Grubb, R. N., and Wait, J. R., 1971, In situ measurements of the complex propagation constant in rock for frequencies from 1 MHz to 10 MHz: Electronics Letters, v. 7, no. 17, p. 506-507, 25 August.

Howell, B. F., Jr., and Licastro, P. H., 1961, Dielectric behavior of rocks and minerals: Am. Mineralogist, v. 46, nos. 3-4, p. 269-288.

Judy, M. M., and Eberle, W. R., 1969, A laboratory method for the measurement of the dielectric constant of rock and soil samples in the frequency range 10^2-10^8 Hertz: Air Force Weapons Laboratory Tech. Rept. no. AFWL-TR-69-41, 34 p.; available from AFWL (WLRP), Kirtland AFB, New Mexico 87117.

Keller, G. V., and Frischknecht, F. C., 1966, Electrical methods in geophysical prospecting: New York, Pergamon Press, 519 p.

Keller, G. V., and Licastro, P. H., 1959, Dielectric constant and electrical resistivity of natural-state cores: U.S. Geol. Survey Bull. 1052-H, p. 257-285.

Khalafalla, A. S., 1971, Dielectric relaxation and rock geophysical characteristics: Honeywell, Inc., Semiann. Rept. no. 12288-IR 1, 59 p. (St. Paul, Minn.)

Lynch, E. J., 1962, Formation evaluation: New York, Harper and Row, 422 p.

Madden, T. R., and Marshall, D., 1958, A laboratory investigation of induced polarization: Massachusetts Inst. Technology RME 3156, (report to the AEC) 115 p.

_____1959a, Electrode and membrane polarization: Massachusetts Inst. Technology RME 3157, (report to the AEC), 78 p.

Madden, T. R., and Marshall, D., 1959b, Induced polarization--a study of its causes and magnitudes in geologic materials: Massachusetts Inst. Technology, RME 3160, (report to the AEC), 80 p.

Scott, J. H., Carroll, R. D., and Cunningham, D. R., 1967, Dielectric constant and electrical conductivity measurements of moist rock--A new laboratoy method: Jour. Geophys. Research, v. 72, no. 20, p. 5101-5115.

Smith-Rose, R. L., 1933, The electrical properties of soil for alternating currents at radio frequencies: Royal Soc. London Proc., Ser. A, v. 140, p. 359-377.

Valeev, K. A., and Parkhomenko, 1965, Electrical properties of rocks in constant and alternating electric fields: Physics of the Solid Earth, no. 12, p. 803-806.

Von Hippel, A. R., 1954, Dielectrics and waves: New York, John Wiley and Sons, 284 p.

Waagé, K. M., 1961, Stratigraphy and refractory clayrocks of the Dakota group along the northern Front Range, Colorado: U.S. Geol. Survey Bull. 1102, 154 p.

Ward, S. H., and Fraser, D. C., 1968, Conduction of electricity in rocks, Chap. 2, pt. B, v. 2 of Mining Geophysics: Oklahoma Soc. Exploration Geophysicists, p. 197-223.

Winsauer, W. O., and McCardell, W. M., 1953, Ionic double-layer conductivity in reservoir rock: Petroleum Trans., AIME, v. 198, p. 129-134.

Wyllie, M. J. R., 1963, The fundamentals of well log interpretation: New York, Academic Press, 238 p.

APPENDIX

Table A1.--Resistivity of Sunnyside sandstone as a function of frequency.

Sample number	ρ_w	S_w	Frequency in Hertz						
			10^2	10^3	10^4	10^5	10^6	10^7	10^8
1111	625.0	1.000	343	330	317	306	282	219	80.2
1112	100.0	1.000	296	287	280	275	254	200	62.7
1121	30.0	1.000	198	191	185	180	171	139	53.2
1123	10.0	1.000	93.2	89.6	87.1	84.7	82.2	74.8	34.9
1133	10.0	1.000	73.7	71.5	69.7	68.1	65.9	60.7	31.3
1133	10.0	.606	108	104	101	99.4	94.3	84.2	41.7
1133	10.0	.591	106	102	100	97.5	93.2	82.5	41.0
1133	10.0	.410	166	161	160	153	143	121	55.3
1133	10.0	.308	214	206	200	195	184	153	64.6
1133	3.0	1.000	34.7	33.9	33.3	32.8	31.9	30.0	16.1
1112	1.0	1.000	14.9	14.7	14.6	14.4	14.1	13.6	8.03
1114	1.0	1.000	12.8	12.6	12.5	12.4	12.2	11.9	7.53
1112	1.0	.670	27.1	26.7	26.4	26.0	25.4	24.3	13.4
1114	1.0	.650	21.1	20.8	20.6	20.5	19.9	19.0	10.7
1114	1.0	.602	26.2	25.8	25.5	25.2	24.5	23.1	12.7
1114	1.0	.500	44.7	43.9	43.3	42.9	41.5	38.6	20.3
1131	1.0	.470	43.4	42.6	42.0	41.8	40.4	37.6	20.1
1114	1.0	.380	55.6	54.8	53.9	52.8	52.0	45.8	23.4
1121	.3	1.000	4.12	4.10	4.12	4.10	4.01	3.90	2.97

Table A2.--Dielectric constant of Sunnyside sandstone as a function of frequency.

Sample number	ρ_w	S_w	Frequency in Hertz						
			10^2	10^3	10^4	10^5	10^6	10^7	10^8
1111	625.0	1.000	14600	1430	161	42.1	19.0	15.9	13.5
1112	100.0	1.000	14100	1210	127	34.4	18.3	15.5	13.7
1121	30.0	1.000	22900	2030	194	41.5	18.1	15.4	13.7
1123	10.0	1.000	42500	3820	384	112	20.4	16.0	14.3
1133	10.0	1.000	53100	4420	396	64.2	21.7	17.0	14.0
1133	10.0	.606	41700	3510	312	52.9	17.9	12.6	9.74
1133	10.0	.591	38900	3260	288	53.6	19.0	12.9	9.89
1133	10.0	.410	26500	2220	366	78.4	16.5	10.8	7.56
1133	10.0	.308	19700	1860	176	56.2	14.4	9.72	6.63
1133	3.0	1.000	85200	7540	658	72.5	25.6	16.8	15.1
1112	1.0	1.000	108000	8830	824	33.3	28.6	17.2	16.4
1114	1.0	1.000	121000	9860	950	132	31.8	25.0	16.4
1112	1.0	.670	64800	5610	563	85.5	23.0	14.6	11.2
1114	1.0	.650	81300	6670	542	104	25.8	14.9	12.1
1114	1.0	.602	64100	5470	474	91.7	25.2	14.8	10.7
1114	1.0	.500	41500	3790	429	68.8	20.0	12.0	8.10
1131	1.0	.470	54700	4570	457	63.4	18.4	12.1	8.39
1114	1.0	.380	32600	3040	372	65.6	22.1	11.9	7.48
1121	.3	1.000	220000	11000	1270	240	46.1	21.8	35.8

Table A3.--Resistivity of Lyons Sandstone as a function of frequency.

Sample number	ρ_w	S_w	Frequency in Hertz						
			10^2	10^3	10^4	10^5	10^6	10^7	10^8
12312	95.0	1.000	237	234	232	229	220	171	59.8
12306	87.0	1.000	207	204	202	198	189	149	52.3
12318	63.0	1.000	211	206	203	199	185	146	53.2
12304	10.0	1.000	63.4	62.0	60.9	59.4	57.1	52.8	28.3
12304	10.0	1.000	69.0	68.0	66.9	65.8	61.0	50.0	26.9
12307	10.0	.660	93.1	91.4	89.6	87.6	83.7	73.0	39.3
12307	10.0	.398	136	133	130	127	112	102	52.2
12317	3.0	1.000	28.6	28.5	28.1	27.8	26.5	25.5	14.6
12303	3.0	1.000	32.1	31.7	31.2	31.1	29.7	28.1	15.7
12303	3.0	.665	58.5	57.7	57.0	56.3	53.9	45.1	25.0
12303	3.0	.372	76.7	75.4	74.1	71.7	69.2	64.1	----
12302	1.0	1.000	12.1	12.0	11.9	11.9	11.8	11.3	7.04
12314	1.0	1.000	12.2	12.1	12.0	11.9	11.7	11.4	6.96
12314	1.0	.625	24.4	24.1	23.9	23.7	22.7	22.0	13.2
12314	1.0	.320	43.1	42.7	42.3	41.9	40.1	39.3	23.4
12314	1.0	.230	66.7	66.0	65.2	64.6	62.7	59.4	34.0
12321	.3	1.000	4.11	4.10	4.08	4.11	4.03	3.97	2.84
12311	.3	1.000	4.08	4.07	4.06	4.08	4.00	3.83	2.72
12311	.3	.660	7.26	7.32	7.26	7.16	7.07	6.92	4.60
12311	.3	.319	17.1	17.1	16.9	16.7	16.4	16.0	9.82

Table A4.--Dielectric constant of Lyons Sandstone as a function of frequency.

Sample number	ρ_w	S_w	Frequency in Hertz						
			10^2	10^3	10^4	10^5	10^6	10^7	10^8
12312	95.0	1.000	6720	534	65.5	34.5	19.1	16.5	13.4
12306	87.0	1.000	7430	630	79.9	38.0	32.3	16.7	13.5
12318	63.0	1.000	11400	941	106	44.4	21.2	15.8	12.4
12304	10.0	1.000	41200	3570	386	78.7	23.8	15.2	12.4
12304	10.0	1.000	36900	3080	295	96.0	38.9	15.4	11.3
12307	10.0	.660	27200	2570	321	66.7	34.7	12.4	9.65
12307	10.0	.398	18900	1920	240	52.8	17.6	9.70	6.95
12317	3.0	1.000	64700	5790	642	78.3	24.1	15.3	13.8
12303	3.0	1.000	56500	4760	432	65.3	23.0	14.5	13.0
12303	3.0	.665	34200	3000	355	76.8	30.2	13.9	8.95
12303	3.0	.372	31700	2180	317	58.6	15.4	9.77	----
12302	1.0	1.000	77400	5600	577	95.7	26.0	16.6	16.5
12314	1.0	1.000	75000	5400	590	91.0	23.3	14.7	15.6
12314	1.0	.625	46600	3730	422	75.2	34.7	13.3	9.26
12314	1.0	.320	32900	2580	255	58.9	13.6	8.74	6.23
12314	1.0	.230	23000	1960	203	50.7	11.8	7.86	5.39
12321	.3	1.000	124000	5590	860	168	14.9	14.7	29.7
12311	.3	1.000	115000	5740	884	166	12.4	16.5	33.9
12311	.3	.660	67500	4780	649	90.0	37.8	14.4	17.9
12311	.3	.319	37300	3420	388	71.9	15.2	9.49	7.16

Table A5.--Resistivity of Laramie sandstone as a function of frequency--Continued

Sample number	ρ_w	S_w	Frequency in Hertz						
			10^2	10^3	10^4	10^5	10^6	10^7	10^8
1302	3.0	0.890	25.6	24.9	24.3	23.8	22.3	20.9	13.4
1320	3.0	.830	26.7	26.1	25.5	24.9	23.5	22.3	14.1
1320	3.0	.680	34.3	33.5	32.5	31.9	30.3	28.1	15.1
1310	1.0	1.000	10.8	10.7	10.6	10.6	10.3	9.84	6.13
1319	1.0	1.000	9.75	9.54	9.45	9.35	9.08	8.69	5.69
1319	1.0	.910	10.9	10.7	10.6	10.6	10.1	9.69	6.10
1304	1.0	.770	13.9	13.7	13.5	13.3	13.0	12.3	7.39
1319	1.0	.740	14.6	14.4	14.1	13.9	13.6	13.0	8.54
1304	1.0	.630	22.5	22.0	21.6	22.2	20.7	19.1	10.1
1312	.3	1.000	3.37	3.35	3.34	3.35	3.25	3.17	2.69
1314	.3	1.000	3.11	3.14	3.12	3.07	3.07	3.00	2.49
1314	.3	.910	3.47	3.44	3.42	3.43	3.34	3.27	2.59
1312	.3	.810	4.29	4.27	4.24	4.16	4.15	4.04	3.02
1314	.3	.760	4.83	4.78	4.73	4.72	4.60	4.48	3.18
1312	.3	.690	6.02	5.98	5.95	5.90	5.77	5.62	4.00

Table A6.--Dielectric constant of Laramie sandstone as a function of frequency.

Sample number	ρ_w	S_w	Frequency in Hertz						
			10^2	10^3	10^4	10^5	10^6	10^7	10^8
1313	500.0	1.000	255000	1860	186	62.0	31.2	21.6	16.2
1313	441.0	1.000	21000	1570	145	58.8	35.6	12.2	17.7
1306	100.0	1.000	34900	2590	234	63.2	32.2	23.7	18.0
1307	100.0	1.000	36200	2640	233	64.7	31.7	23.5	18.0
1318	30.0	1.000	59800	4160	381	85.1	31.6	23.2	18.5
1316	30.0	1.000	51800	3960	358	82.2	30.9	22.9	18.2
1303	10.0	1.000	64700	5740	664	123	37.0	22.8	18.8
1315	10.0	1.000	69100	5720	559	109	33.5	21.6	18.2
1303	10.0	.920	45300	4020	438	170	38.3	20.6	14.9
1303	10.0	.810	59100	5800	700	190	33.9	19.4	14.8
1315	10.0	.806	56500	4810	486	165	29.1	18.5	14.3
1315	10.0	.680	50200	4650	523	160	26.8	16.5	12.3
1302	3.0	1.000	105000	10400	1110	192	43.7	22.7	19.1
1320	3.0	1.000	112000	10200	1020	174	42.9	22.9	19.4
1302	3.0	.890	103000	10300	1110	187	30.2	21.8	16.6
1320	3.0	.830	99900	9180	896	154	37.2	19.6	15.1

Distribution:

Capt. L. West, AFWL/WLRE (30)
Kirtland Air Force Base, New Mexico

U.S. Geological Survey, Washington, D. C.:
R. B. Raup
V. E. McKelvey
Military Geology Branch
Chief Hydrologist, WRD (Attn: Radiohydrology Section)

U.S. Geological Survey, Mercury, Nevada:
Geologic Data Center (5)